arXiv:1304.0075v1 [cond-mat.mtrl-sci] 30 Mar 2013

Theoretical Study of the Ground and Low-Lying Excited States of Long Acenes

Himanshu Chakraborty and Alok Shukla

Department of Physics, Indian Institute of
Technology Bombay, Powai, Mumbai 400076, INDIA[*]

Abstract

Several years back Angliker *et al*. [Chem. Phys. Lett. **87**, 208 (1982)] predicted nonacene to be the first linear acene with the triplet state 1^3B_{2u} as the ground state, instead of the singlet 1^1A_g state. However, contrary to that prediction, in a recent experimental work Tönshoff and Bettinger [Angew. Chem. Int. Ed. **49**, 4125 (2010)] demonstrated that nonacene has a singlet ground state. Motivated by this experimental finding, we decided to perform a systematic theoretical investigation of the triplet states of polyacenes, with an emphasis on singlet-triplet splitting, starting from naphthalene, all the way up to decacene. Methodology adopted in our work is based upon Pariser-Parr-Pople model (PPP) Hamiltonian, along with large-scale multi-reference singles-doubles configuration interaction (MRSDCI) approach. Our results predict that the singlet-triplet gap decreases with acene size and octacene onwards, it reaches saturation. Thus no singlet-triplet crossover takes place in longer acenes and the ground state is of singlet multiplicity. We also analyze the nature of many-particle wavefunction of the correlated singlet ground state and find that the longer acenes exhibit tendency towards a open-shell singlet diradical ground state. Moreover, when we compare the experimental absorption spectra of octacene and nonacene with their calculated singlet and triplet absorption spectra, we observe very good agreement for the singlet case. Hence, the optical absorption results also confirm the singlet nature of the ground state for longer acenes. Calculated triplet absorption spectra of acenes predict two well separated intense long-axis polarized absorptions, as against one such peak observed for the singlet case. This is in important prediction regarding the triplet optics of acenes, which can be tested in future experiments on oriented samples.

PACS numbers: 78.30.Jw, 78.20.Bh, 42.65.-k

I. INTRODUCTION

Polyacenes, which can be seen as linearly fused benzene rings, are known for their well defined structures, and crystalline forms.[1,2] Because of their small band gaps and high charge-carrier mobilities, they find potential applications in novel opto-electronic devices such as light-emitting diodes, and field effect transistors *etc.,* which make them experimentally and theoretically a very important class of materials.[3,4] In spite of a long tradition of research,[5] the field of acenes has experienced a resurgence of interest in recent years because they are also perceived as the building blocks for organic electronic materials such as graphene nanoribbons.[3,6]

Although pentacene, has excellent optical and transport properties, however, it is conceivable that the longer acenes could have even more attractive properties, with possible applications in the field of nanotechnology.[6] As the size of the longer acenes approaches the nanometer scale, their reactivity also increases, and, therefore, it has been difficult to synthesize them from heptacene onwards.[7] Recently, many efforts have been made to synthesize the longer acenes, *e.g.*, heptacene and its functionalized derivatives have been synthesized by several workers.[8–12] By using cryogenic matrix-isolation technique, and a protection group strategy, octacene and nonacene have been synthesized by Tönshoff and Bettinger[13], while Kaur *et al.*[14] prepared functionalized nonacene.

While all the known oligoacenes ranging from naphthalene to hexacene have a singlet ground state,[15] some years back, based on an extrapolation of the experimental singlet-triplet gap of the acenes up to pentacene, Angliker *et al.*[15] predicted nonacene to be the first linear acene with a triplet state (1^3B_{2u}) as the ground state, instead of the singlet one (1^1A_g). This was an interesting prediction because, if true, it could open the possibilities of magnetic applications of longer acenes. However, contrary to that prediction, based upon their recent optical absorption experiments, Tönshoff and Bettinger[13] demonstrated that nonacene has a singlet ground state. Motivated by this experimental finding, we decided to perform a systematic theoretical investigation of the electronic structure of the ground and low-lying excited states of longer acenes, with an emphasis on the singlet-triplet splitting, and their optical properties. In order to realize the possible potential of longer acenes in nanotechnology, a deep theoretical understanding of their electronic structure is very important. For our calculations, we adopt a methodology based upon Pariser-Parr-Pople model (PPP) Hamiltonian, along with large-scale multi-reference singles-doubles configuration interaction (MRSDCI) approach. We present results on the singlet and triplet low-lying excited states of octacene, nonacene, and decacene, along with their optical absorption spectra. The calculated spectra are compared with the experimental ones for octacene and nonacene, and excellent agreement is found between our singlet optical absorption spectra, and the experimental ones. This, along with our results on singlet-triplet splitting, leads us to conclude that the acenes in question possess singlet ground states. We also make important predictions about triplet absorption in long acenes, which can be tested in future experiments.

The remainder of this paper is organized as follows. In Section II we briefly review the theoretical methodology adopted in this work. In Section III we present and discuss our results of: (a) the singlet-triplet splitting of oligoacenes of increasing lengths, (b) singlet linear absorption spectra, (c) triplet optical absorption spectra, and (d) the comparison of the experimental absorption spectra of octacene and nonacene, with their calculated spectra. Finally, in Section IV we summarize our conclusions, and present possible directions for the future research work.

II. THEORY

The schematic structures of higher polyacenes studied in this work are shown in 1. The molecule is assumed to lie in the xy-plane, with the conjugation direction taken to be along the x-axis. The carbon-carbon bond length has been fixed at 1.4 Å , and all bond angles have been taken to be 120^o. The reason of choosing this symmetric geometry, against various other possibilities has already been discussed in our earlier paper.[16,17] It can be noted that these structures can also be seen as two polyene chains of suitable lengths, coupled together along the y-direction.

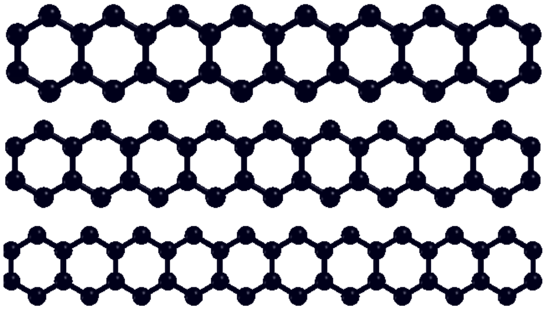

Figure 1. Schematic drawings of long acenes (octacene to decacene, from top to bottom) considered in this work. The x axis is assumed along the conjugation direction, while the y axis is perpendicular to it, in the plane of the figure.

The correlated calculations are performed using the PPP model Hamiltonian, which can be written as

$$H = H_{C_1} + H_{C_2} + H_{C_1C_2} + H_{ee},$$

where H_{C_1} and H_{C_2} are the one-electron Hamiltonians for the carbon atoms located on the upper and the lower polyene like chains, respectively. $H_{C_1C_2}$ is the one-electron hopping between the two chains, and H$_{ee}$ depicts the electron-electron repulsion. The individual terms can now be written as,

$$H_{C_1} = -t_0 \sum_{\langle k,k' \rangle} B_{k,k'},$$

$$H_{C_2} = -t_0 \sum_{\langle \mu,\nu \rangle} B_{\mu,\nu},$$

$$H_{C_1C_2} = -t_{\perp} \sum_{\langle k,\mu \rangle} B_{k,\mu}.$$

$$H_{ee} = U \sum_i n_{i\uparrow} n_{i\downarrow} + \frac{1}{2} \sum_{i \neq j} V_{i,j}(n_i - 1)(n_j - 1).$$

In the equation above, k, k' are carbon atoms on the upper polyene chain, μ, ν are carbon atoms located on the lower polyene chain, while i and j represent all the atoms of the oligomer. Symbol $\langle ... \rangle$ implies nearest neighbors, and $B_{i,j} = \sum_{\sigma}(c^{\dagger}_{i,\sigma}c_{j,\sigma} + h.c.)$, where $c^{\dagger}_{i,\sigma}$ $(c_{i,\sigma})$ denotes the creation (annihilation) operator for a π orbital of spin σ, located on the ith carbon atom. Matrix elements t_0, and $t_{\perp}$ depict one-electron hops. As far as the values of the hopping matrix elements are concerned, we took $t_0 = 2.4$ eV for all nearest neighbor hopping with $t_{\perp} = t_0$, consistent with the undimerized ground state for polyacene argued by Raghu *et al.*[18]

The Coulomb interactions are parametrized according to the Ohno relationship,[19]

$$V_{i,j} = U/\kappa_{i,j}(1 + 0.6117R^2_{i,j})^{1/2} \ ,$$

where, $\kappa_{i,j}$ depicts the dielectric constant of the system which can simulate the effects of screening, U is the on-site repulsion term, and $R_{i,j}$ is the distance in Å between the ith and the jth carbon atoms. In the present work, we have performed calculations using "standard parameters"[19] with $U = 11.13$ eV and $\kappa_{i,j} = 1.0$, as well as "screened parameters"[20] with $U = 8.0$ eV and $\kappa_{i,j} = 2.0$ $(i \neq j)$ and $\kappa_{i,i} = 1.0$. The screened parameters employed here were devised by Chandross and Mazumdar[20] with the aim of accounting for the inter chain screening effects in phenylene based polymers. Our motive behind using these parameters is precisely the same.

The starting point of the correlated calculations for the molecules is the Restricted Hartree-Fock (RHF) calculations, employing the PPP Hamiltonian, using a code developed in our group.[21] All the resultant HF molecular orbitals are treated as active orbitals. The many-body effects beyond RHF are computed using the Multi-Reference Singles Doubles Configuration Interaction (MRSDCI) method[22–25] in the following manner. After RHF calculations of the ground state 1^1A_g, the MRSDCI calculation of the ground state, 1^1A_g and excited states of symmetries $^1B_{2u}$ and $^1B_{3u}$ are performed by taking the lowest energy configuration of the corresponding symmetry ($1B_{2u}$ is $H \rightarrow L$ and $1B_{3u}$ is $H \rightarrow L+1$ and $H-1 \rightarrow L$, where H and L corresponds to Highest Occupied Molecular Orbital (HOMO) and Lowest Unoccupied Molecular Orbital (LUMO)). A similar approach is adopted for the triplet states as well, except that one has to ensure that the multiplicity of the wave functions is triplet. From the CI calculations, we obtain the eigenfunctions and eigenvalues corresponding to the correlated ground and excited states of the examined molecules. Using these eigenfunctions, the dipole matrix elements between the ground state and various excited states are computed. For the triplet states, the matrix elements are calculated with respect to the lowest triplet state 1^3B_{2u}. These dipole matrix elements, along with the energies of the excited states are, in turn, utilized to calculate linear (or triplet) optical absorption spectrum. Important excited states contributing to various peaks of the spectrum are identified, and a new set of MRSDCI calculations are performed with an increased number of reference configurations contributing both to the ground state, and the excited states, leading to a new absorption spectrum. This procedure is iterated until the computed spectrum converges satisfactorily.

III. RESULTS AND DISCUSSIONS

In this section we present the results of our MRSDCI calculations on polyacenes ranging from naphthalene to decacene examining their singlet-triplet gaps, with the aim of determining the spin-multiplicity of their ground state. Furthermore, we also present calculations on the optical absorption of the long acenes, namely, octacene to decacene from their lowest triplet states (1^3B_{2u}), and the lowest-singlet state (1^1A_g), and compare the results with the experimental ones, where available.

A. Singlet-Triplet Splitting

The first set of calculations which we performed to explore singlet-triplet (1^1A_g-1^3B_{2u}) splitting in oligoacenes were at the RHF level for the singlet states, and the UHF (Unrestricted Hatree Fock) level for the triplet states. For an oligomer containing $2m$ electrons, in the UHF calculations $m+1$ electrons were assigned the majority spin, and the remaining $m-1$ electrons the minority spin to represent the triplet ground state. The results of these calculations for oligoacenes up to acene-15 (acene-n denotes an oligomer with n benzene rings) are presented in I. Examining the values of the singlet-triplet splitting $\Delta E = E(1^3B_{2u}) - E(1^1A_g)$ for various oligomers, it is obvious that: (a) in standard-parameter based calculations, acene-10 onwards triplet state become lower in energy as compared to the singlet state, while, (b) with screened parameters, this crossover takes place at smaller lengths, starting with acene-7. Therefore, these results appear to confirm the essential prediction of Angliker *et al.*[15] that the singlet-triplet crossover will take place in oligoacenes with the increasing lengths, although, they differ in details in that Angliker *et al.*[15] predicted the crossover from acene-9 onwards. However, the shortcomings of these calculations are that they have been performed at the mean-field level, and, therefore, do not include the electron-correlation effects. Although, the calculations of Angliker *et al.*[15] were performed using the CI approach, but they employed the singles-CI (SCI) method, which accounts for the electron-correlation effects in a very limited manner. Furthermore, another calculation, performed by Houk *et al.*,[26] also predicted the singlet-triplet crossover in oligoacenes. However, that calculation was performed using an *ab initio* DFT based approach,[26] and, therefore, did not account for the electron-correlation effects. Based upon past calculations,[27] it is a well-known fact that in order to be able to predict the correct excited state orderings in conjugated polymers, it is very important to account for the electron-correlation effects in an accurate manner. Therefore, we decided to go beyond the HF approach, and performed large-scale CI calculations to explore the singlet-triplet ordering in polyacenes. Before we present and discuss our results, we would like to give a flavor to the reader as to the size of the CI calculations performed. II presents the number of reference states used in the MRSDCI calculations, and the total size of the resultant CI matrix. The largest calculation consisted of more than one million configurations, from which it is obvious that our calculations were large scale, and, thus, they account for the electron-correlation effects in an adequate manner. The calculated values of the singlet-triplet gap, and their comparison with the experimental and other theoretical calculations, are presented in III, for the oligoacenes ranging from naphthalene to decacene. The variation of the singlet-triplet gap, as a function of the oligomer length, is presented in 2. It is obvious both from the table, and the figure, that the excitation energy of 1^3B_{2u} state decreases as the oligomer length increases. Nevertheless, even for decacene the singlet-triplet gap is nonvanishing, and appears to saturate as a function of the increasing chain length. As is obvious from the 2 that similar trends were also observed in the works of other authors, except the DFT-based UB3LYP calculation performed by Bendikov *et al.*[28] which reports much smaller singlet-triplet gaps. We believe that these smaller gaps obtained in the work of Bendikov *et al.*,[28] could be attributed to the well-known tendency of DFT to underestimate the energy gaps.

Therefore, based upon the fact that for decacene our screened parameter based calculations predict a singlet-triplet gap ≈ 0.5 eV, we conclude that even for longer acenes, the singlet state 1^1A_g will be the ground state, and thus no singlet-triplet crossover of the kind predicted by Angliker *et al.*,[15] occurs as per our calculations. As far as comparison with other authors is concerned, our screened parameter results are in good quantitative agreement with DMRG/STO-3G[29] results, and good qualitative agreement with the DMRG/DZ results.[29] Recently, Hajgato *et al.*[30] performed first principles coupled cluster CCSD(T) calculations on the singlet-triplet gaps of acenes ranging from octacene to undecacene (acene-11), and their reported value of 0.58 eV for octacene is in perfect agreement with our screened parameter results. However, for nonacene and decacene their reported values 0.46 eV and 0.35 eV[30], respectively, are smaller than our screened parameter values of 0.56 eV and 0.54 eV. Regarding the singlet-triplet gap in the polyacene limit ($n \rightarrow \infty$), Raghu *et al.*,[31] using the DMRG method and the PPP model, predicted it to be 0.53 eV, while Gao *et al.,*[32] using a spin Hamiltonian, estimated it to be 0.446 eV, both of which are close to our screened-parameter value of 0.5 eV computed for decacene.

Bendikov *et al.*[28] noted that the restricted singlet density functional ground state of higher acenes would become unstable due to its open-shell nature, with two unpaired electrons (a singlet diradical[33]) for acenes longer than hexacene. Based upon *ab initio* DMRG calculations on acenes in the range n = 2-12, Chan and coworkers found that the ground state wave functions for longer acenes were of the type of polyradical singlets.[29] In an another DFT work, Jiang and Dai[34] predicted the ground state of octacene and higher acenes to be antiferromagnetic (in other words, open-shell singlet), but not necessarily a diradical. Unlike the DFT calculations, in our approach, the many-body wave functions of the ground state and the excited states of the studied oligomers are available. Therefore, we decided to probe the nature of the ground state of longer acenes to ascertain whether, or not, they exhibit a polyradical character. The character of the many-body wave functions of the 1^1A_g ground state, obtained in our best CI calculations on oligomers ranging from naphthalene to decacene are presented in IV, for both the standard, and the screened parameters. From the results, it is obvious that the contribution of the configurations with two open-shell orbitals increases with respect to the HF reference state with the increasing oligomer length, while the contribution of the closed-shell HF state decreases. Therefore, based upon our results, we conclude that the longer acenes do exhibit a tendency towards a singlet diradical ground state.

n	std			scr		
	S	T	ΔE	S	T	ΔE
2	-22.73	-20.02	-2.70	-19.19	-17.09	-2.10
3	-31.98	-30.36	-1.61	-27.17	-26.01	-1.16
4	41.16	-40.14	-1.02	-35.10	-34.48	-0.62
5	-50.32	-49.70	-0.62	-43.02	-42.72	-0.29
6	-59.47	-59.10	-0.37	-50.94	-50.85	-0.08
7	-68.62	-68.41	-0.21	-58.85	-58.89	0.04
8	-77.76	-77.67	-0.10	-66.76	-66.89	0.13
9	-86.91	-86.88	-0.02	-74.67	-74.86	0.18
10	-96.05	-96.07	0.02	-82.59	-82.81	0.22
11	-105.19	-105.24	0.05	-90.50	-90.74	0.24
12	-114.34	-114.41	0.07	-98.41	-98.67	0.25
13	-123.48	-123.56	0.08	-106.32	-106.59	0.26
14	-132.62	-132.71	0.09	-114.23	-114.50	0.27
15	-141.76	-141.86	0.10	-122.15	-122.42	0.27

Table I. RHF (singlet, S) and UHF (triplet, T), total energies along with their difference in energies (ΔE), in eV, of acenes n=1-15 computed using the standard (std), and the screened (scr) parameters.

Table II. The number of reference configurations (N_{ref}) and the total number of configurations (N_{total}) involved in the MRSDCI (or FCI or QCI, where indicated) calculations, for different symmetry subspaces of various oligoacenes.

n	A_g		$^1B_{2u}$		$^3B_{2u}$	
	N_{ref}	N_{total}	N_{ref}	N_{total}	N_{ref}	N_{total}
2	1[a]	4936[a]	1[a]	4794[a]	1[a]	4816[a]
3	1[a]	623576[a]	1[a]	618478[a]	1[a]	620928[a]
4	1[b]	193538[a]	1[b]	335325[a]	100[c]	323063[c]
					86[d]	319005[d]
5	1[b]	1002597[b]	1[b]	1707243[a]	52[c,d]	581702[c,d]
6	100[c]	1110147[c]	100[c]	1173212[c]	65[c]	1461526[c]
	100[d]	1177189[d]	100[d]	1328252[d]	63[d]	1551590[d]
7	35[c]	856788[c]	30[c]	674925[c]	33[c]	1369624[c]
	22[d]	615590[d]	30[d]	850627[d]	29[d]	1300948[d]
8	18[c]	768641[c]	14[c]	509119[c]	19[c]	1066355[c]
	12[d]	540651[d]	4[d]	145978[d]	14[d]	918645[d]
9	13[c]	959737[c]	13[c]	769387[c]	18[c]	1626229[c]
	12[d]	871397[d]	3[d]	186651[d]	12[d]	1152071[d]
10	11[c]	1202681[c]	12[c]	1192394[c]	15[c]	1735352[c]
	11[d]	1199887[d]	3[d]	270187[d]	10[d]	1318156[d]

[a] FCI method with standard as well as screened parameters,

[b] QCI method with standard as well as screened parameters,

[c] using standard parameters,

[d] using screened parameters.

Table III. For various oligomers, the comparison of the calculated singlet-triplet gaps (excitation energies of 1^3B_{2u}, with respect to the 1^1A_g) with the experiments, and other theoretical results. The column std (scr) corresponds to the results obtained using the standard (screened) parameters in the PPP model Hamiltonian.

n	$E(1^3B_{2u}) - E(1^1A_g)$ (eV)			
	std	scr	Expt.	Other Theoretical
2	2.53	2.11	2.64[35]	2.71[26], 2.72[28], 2.67[29]
3	1.73	1.48	1.87[36]	1.81[26], 1.81[28],1.99[29]
4	1.25	1.11	1.27[37]	1.20[26], 1.16[28],1.51[29]
5	0.99	0.93	0.86 ± 0.03[38]	0.78[26], 0.76[28],1.16[29]
6	0.87	0.85	0.54 ± 0.05[15]	0.46[26], 0.47[28],0.91[29]
7	0.73	0.69	-	0.24[26]
8	0.68	0.58	-	0.07[26], 0.13[28],0.62[29],0.58[30]
9	0.60	0.56	-	0.07[28],0.50[29],0.46[30]
10	0.57	0.54	-	0.11[28],0.46[29],0.35[30]

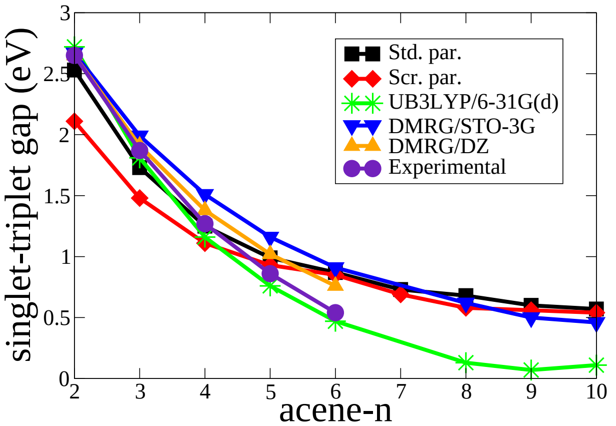

Figure 2. (Color online) Singlet-triplet energy gap as a function of the acene lengths.

Table IV. Magnitudes of the coefficients of the closed-shell Hartree Fock (HF), and the open shell (OS) doubly excited virtual configuration $|H \to L;\, H-1 \to L+1\rangle$ to the singlet 1^1A_g ground state CI wave functions of acene-n, obtained using the standard (std), and the screened (scr) parameters in the PPP model. In the preceding expression H stands for the highest occupied molecular orbital (HOMO), while L stands for lowest unoccupied molecular orbital (LUMO).

n	HF		OS	
	std	scr	std	scr
2	0.94	0.90	0.14	0.13
3	0.91	0.86	0.13	0.11
4	0.88	0.83	0.11	0.13
5	0.84	0.79	0.13	0.14
6	0.81	0.77	0.15	0.16
7	0.80	0.76	0.17	0.19
8	0.79	0.74	0.18	0.20
9	0.77	0.73	0.19	0.21
10	0.76	0.71	0.20	0.22

B. Singlet Linear Optical Absorption calculations

In an earlier work in our group, we had reported the calculations of linear optical absorption spectra of oligoacenes ranging from naphthalene to heptacene.[16] In this work, we extend our calculations to longer acenes, and present the calculations of linear optical absorption in octacene, nonacene and decacene. In 4, 5 and 6, we present the singlet linear absorption spectra of these oligoacenes from their $1^1A_g^-$ singlet state computed using the standard parameters and the screened parameters. As per dipole selection rules for the D_{2h} symmetry, allowed one-photon transitions from the $1^1A_g^-$ state occur to $^1B_{2u}^+$ ($^1B_{3u}^+$) type states via short-axis (long-axis) polarized photons. As per the convention adopted in this work, the short (long) axis correspond to y (x) directions. The essential states contributing to the linear absorption spectra of various acenes are depicted in 3. The many-particle wave functions of the excited states contributing to various peaks in the spectra are presented in the EPAPS.[39] While plotting the absorption spectra, we have restricted ourselves to states which lie below 6 eV, the estimated value of the ionization potentials of the long acenes.[40]

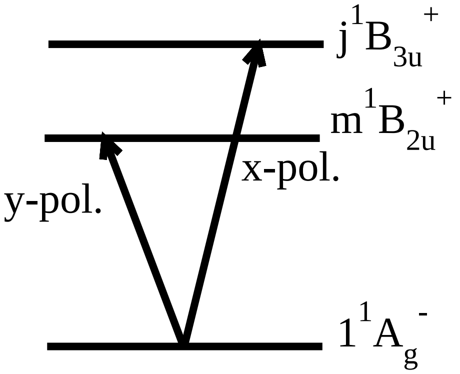

Figure 3. Diagram of the essential states involved in the singlet linear optical absorption in oligoacenes and their polarization characteristics. The arrows connecting two states imply optical absorption, with polarization directions stated next to them. Location of states is not up to scale.

A peak-by-peak detailed description of the computed singlet absorption spectra is provided in the supplementary material.[39] Here we list the salient featurs of the calculated linear optical absorption of octacene, nonacene, and decacene:

1. Quantitatively speaking, screened parameter spectra are redshifted as compared to the standard parameter ones.

2. Most of the intensity is concentrated in the x-polarized (long-axis polarized) spectra originating from the absorption into the $^1B_{3u}^+$ type of states, while the y-polarized (short-axis polarized) absorption into the $^1B_{2u}^+$ type states is comparatively weak. However, a closer examination reveals that most of the intensity in the x-polarized spectrum is derived from the single transition to an $n^1B_{3u}^+$ state (or states which split away from it). If we ignore this transition then the short- and long-axis polarized spectra are of comparable intensity. This aspect of the singlet linear absorption spectrum of long acenes is consistent with what is also observed in the shorter acenes.[16]

3. The first peak corresponds to the y-polarized transition, to the $1^1B_{2u}^+$ excited state of the system. The most important configuration contributing to the many-particle wave function of the state corresponds to $|H \rightarrow L\rangle$ excitation, irrespective of the choice of the Coulomb parameters employed in the PPP model.

4. We have observed that the most intense absorption for the oligoacenes is through an x-polarized photon to a $^1B_{3u}$ state, irrespective of the Coulomb parameters employed in

the calculations. For acene-n, the many-particle wave function of this state exhibits the following general features: (a) for the standard parameter case, single excitations $|H \rightarrow L+n/2-1\rangle + c.c.$, for $n \equiv$ even, and $|H \rightarrow L+(n-1)/2\rangle + c.c.$, for $n \equiv$ odd, dominate the wave function, while (b) with screened parameters the dominant configurations are single excitations $|H \rightarrow L+n/2\rangle + c.c.$ for $n \equiv$ even, and $|H \rightarrow L+(n-1)/2\rangle + c.c.$ for $n \equiv$ odd. The aforesaid difference between the standard and the screened parameters is because of different energetic ordering of the symmetries of the molecular orbitals for the standard and screened parameters.

Figure 4. Singlet linear absorption spectra of octacene computed using: (a) standard parameters and (b) screened parameters. A uniform line width of 0.1 eV was assumed while plotting the spectra. The subscripts attached to the peak labels indicate the polarization directions x and y

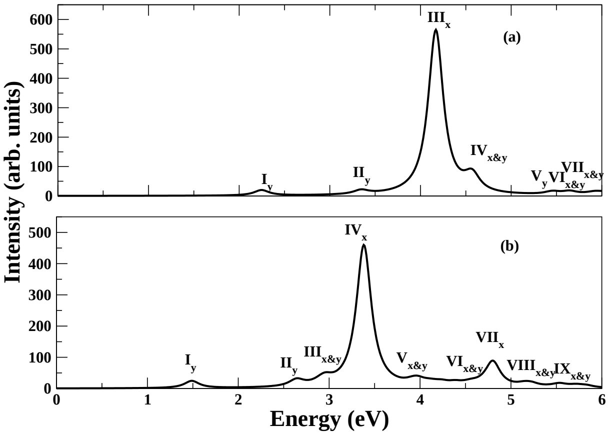

Figure 5. Singlet linear absorption spectra of nonacene computed using: (a) standard parameters and (b) screened parameters. The rest of the information is same as in the caption of 4

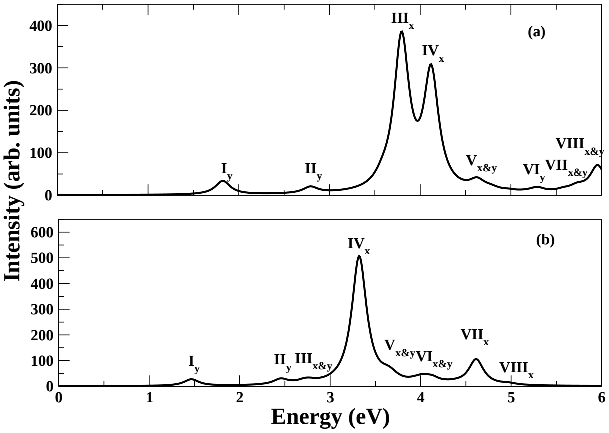

Figure 6. Singlet linear absorption spectra of decacene computed using: (a) standard parameters and (b) screened parameters. The rest of the information is same as in the caption of 4

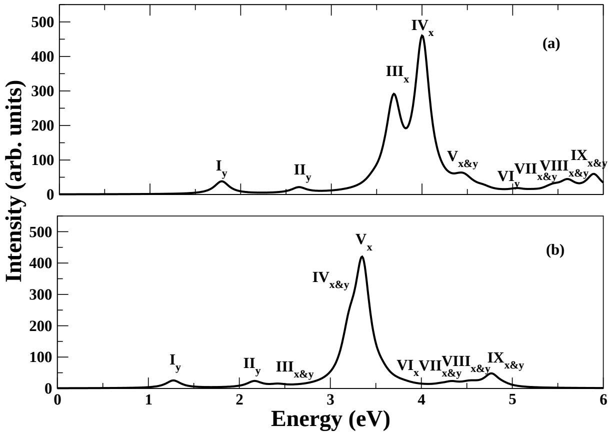

C. Triplet optical absorption calculations

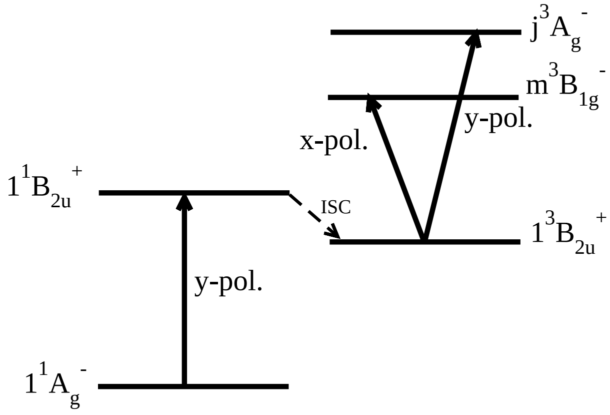

Figure 7. Diagram of the essential states involved in the triplet absorption spectra of oligoacenes, and their polarization characteristics. The arrows connecting two states imply optical absorption, with polarization directions stated next to them. Location of states is not up to scale. ISC refers to inter-system crossing.

In optical absorption experiments, one can probe the triplet excited states because frequently the first singlet excited state S_1 ($1^1B_{2u}^+$, in the present case) decays to the first triplet excited state T_1 ($1^3B_{2u}^+$, in the present case) located below S_1, through nonradiative inter-system crossing (ISC*),* as shown in 7. Once the system reaches the triplet manifold, normal optical absorption experiments can be performed to probe higher triplet states. In the present work, we restrict ourselves to the triplet one-photon absorption spectra of octacene, nonacene, and decacene from their $1^3B_{2u}^+$ state, computed using the MRSDCI method. For the case of oligoacenes, as per electric-dipole selection rules of the D_{2h} point group, the long-axis (x-axis) polarized photons cause transitions from the $1^3B_{2u}^+$ to $^3B_{1g}^-$ type of states, while the short-axis (y-axis) polarized ones lead to the $^3A_g^-$ type states (*cf.* 7). The calculated triplet absorption spectra of these oligoacenes are displayed in 8, 9 and 10, while the wave functions of the excited states contributing to various peaks in the spectra are presented (cf., Ref.[39]). While plotting the triplet absorption spectra, we have been careful to include only those states which lie below 6 eV excitation energy (with respect to the $1^1A_g^-$ state), which is the estimated value of the ionization potentials of the long acenes.[40] A detailed description of the characteristics of various peaks in the calculated triplet absorption spectra of octacene, nonacene, and decacene, is presented in the accompanying supplementary material.[39]) Below we discuss the salient features of our results:

1. Similar to the case of singlet absorption, screened parameter spectra are red shifted as compared to the standard parameter ones.

2. Most of the intensity is concentrated in the x-polarized (long-axis polarized) spectra corresponding to the aborption into the $^3B_{1g}^-$ type of states, while the y-polarized absorption into the $^3A_g^-$ type states is very faint.

3. From 8, 9, and 10 it is obvious that the triplet absorption spectrum is dominated by two intense x-polarized peaks which are well separated in energy ($>$2 eV), irrespective of the oligoacene in question, or the Coulomb parameters employed in the calculations. The first of these peaks is peak I in all the cases, while the second one is either peak IV or V, depending upon the oligoacene, or the Coulomb parameters employed. In the standard parameter based calculations, peak I is always the second most intense peak, while the second of these peaks (IV or V) is the most intense. In the screened parameter calculations the situation is exactly the reverse, with peak I being the most intense, while peak IV or V being the second most intense peak of the spectrum. Peak I always corresponds to the $1^3B_{1g}^-$ excited state of the system, whose wave function is dominated by the single excitations $|H \rightarrow L+1\rangle + c.c.$, irrespective of the oligoacene in question, or the choice of Coulomb parameters. The second intense peak (IV or V) corresponds to a higher $^3B_{1g}^-$ type state of acene-n, whose wave function mainly consists of: (a) for the standard parameters, double excitations $|H \rightarrow L;\, H-(n/2-1) \rightarrow L\rangle + c.c.$ for $n \equiv$ even, and $|H \rightarrow L;\, H-(n-1)/2 \rightarrow L\rangle + c.c.$ for the $n \equiv$ odd case, while (b) for the screened parameters, double excitations $|H \rightarrow L;\, H-n/2 \rightarrow L\rangle + c.c.$ for $n \equiv$ even, and $|H \rightarrow L;\, H-(n-1)/2 \rightarrow L\rangle + c.c.$ for the $n \equiv$ odd case. This difference between the standard and the screened parameter results is because of the different energetic ordering of the molecular orbital symmetries in longer acenes, for the two sets of Coulomb parameters.

4. Other peaks in the spectrum correspond to either x or y polarized transitions to the higher excited states of the system, which are described in detail (cf., Ref.[39]).

Figure 8. Triplet absorption spectra of octacene from the $1^3B_{2u}^+$ state computed using: (a) standard parameters and, (b) screened parameters. A uniform line width of 0.1 eV was assumed while plotting the spectra. The subscripts attached to the peak labels indicate the polarization directions x and y .

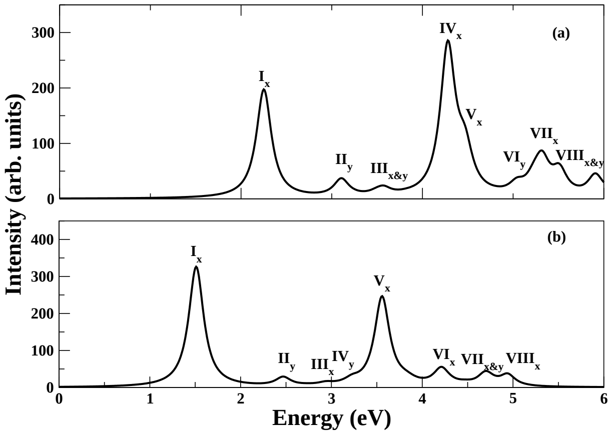

Figure 9. Triplet absorption spectra of nonacene from the $1^3B_{2u}^+$ state computed using: (a) standard parameters and, (b) screened parameters. The rest of the information is same as in the caption of 8.

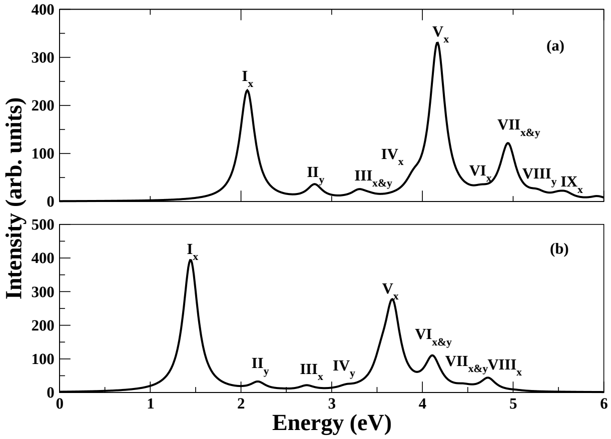

Figure 10. Triplet absorption spectra of decacene from the $1^3B_{2u}^+$ state computed using: (a) the standard parameters and, (b) the screened parameters. The rest of the information is same as in the caption of 8.

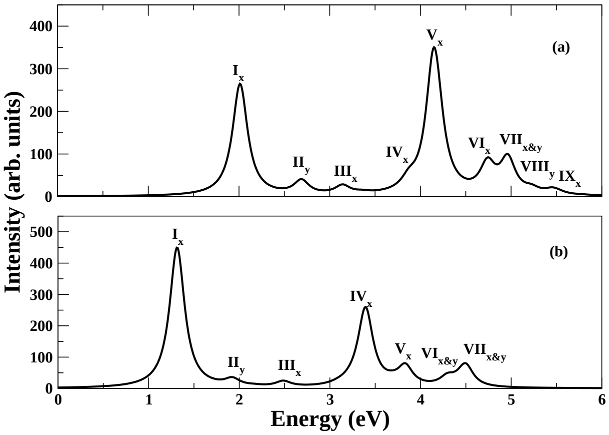

D. Comparison of singlet and triplet absorption calculations of octacene and nonacene with the experimental results

In V, the results of the experimental absorption of octacene and nonacene, reported by Tönshoff and Bettinger,[13] have been presented, showing the excitation energies, relative intensities, and tentative assignments of the UV/vis electronic absorptions. Next, we compare our computed singlet and triplet absorption results, with the expermental ones, in terms of the peak energies (in eV) and relative intensities/oscillator strength. The relative oscillator strength (ROS) in the computed absorption spectra is the ratio of the calculated oscillator strength of a given state, with respect to that of the most intense state. The relative oscillator strengths of the peaks in the calculated absorption spectra are compared with the reported relative intensities (RI) of the corresponding peaks in the experiment spectra.

1. Octacene

Comparing the experimental values of the energies of the absorption peak of octacene from the Va, with our calculated values for the singlet case (cf., Ref.[39]), the lowest state S_1(1.54 - 1.86 eV, RI= 0.025 for the 1.54 eV) of the experimental results matches nicely with the first peak at 1.49 eV (ROS= 0.050) obtained in the screened parameter calculations, than the corresponding one for the standard parameter case located at 2.24 eV. The second state of the experimental results S_2 (2.40 eV, RI=0.02) again agrees much better with the screened parameter result, 2.65 eV (ROS=0.047) than with the standard parameter one located at 3.34 eV. The third state of the experimental results, S_3 (2.54 eV, RI=0.050) has a better agreement with the third state of the screened parameter spectrum 2.97 eV (ROS=0.046), than with corresponding standard parameter peak at 4.17 eV. The most intense peak in the experimental results corresponds to S_7 (3.68-3.78 eV, RI=1.0) lies in between the highest peak of the screened and standard parameter calculations located at 3.38 eV (ROS=1.0), and 4.17 eV (ROS=1.0), respectively. We note that with the increasing peak energy, the agreement between the experiments and theory begins to deteriorate. Nevertheless, even in the worst case scenario of the most intense peak (S_7 of the experiments), the disagreement between the screened parameter results and the experiments is below 10%, as far as the peak location is concerned. This disagreement, which is fairly acceptable from a quantitative aspect, is possibly due to the reduced computational accuracy of our approach because of the high energies of the states involved. As far as the comparison of the experimental results with the triplet absorption calculations (cf., Ref.[39]) is concerned, the first peaks in the computed triplet spectra, 3.04 eV (ROS=0.839) for the standard parameter, and 1.97 eV (ROS=1.0) for the screened parameters, disagree completely with the location of S_1, as well as its relative intensity in the experimental spectrum. The same trend holds for the higher excited states as well. Thus, we conclude that the experimental absorption spectrum of octacene is indeed from the $1^1A_g^-$ ground state of the system, confirming yet again that the ground state of octacene has the singlet multiplicity.

We also note that Raghu *et al.*[31] predicted a very large optical gap of 2.60 eV for octacene, based upon their DMRG calculations, employing the PPP Hamiltonian.

Table V. The experimental values of the wavelengths, relative intensities and tentative assignments of the UV/vis electronic absorptions of octacene (left) and nonacene (right)[13]

E(eV)	I (rel.)	Octacene State
1.54	0.025	S_1
1.69	0.011	
1.73	0.016	
1.86	0.007	
2.40	0.02	S_2
2.54	0.05	S_3
2.72	0.05	
3.16	0.08	S_4
3.29	0.49	S_5
3.33	0.43	
3.48	0.46	S_6
3.68	0.90	S_7
3.78	1.00	

E(eV)	I (rel.)	Nonacene State
1.43	0.020	S_1
1.58	0.006	
1.62	0.016	
2.33	0.033	S_3
2.50	0.023	S_4
2.67	0.030	S_5
2.80	0.048	S_6
2.97	0.19	S_7
3.14	0.52	
3.42	0.14	S_8
3.66	1.00	S_9

2. Nonacene

Similarly, comparing the experimental values of the energies of the absorption peak of nonacene from the Vb, with our calculated values for the singlet case (cf., Ref.[39]), the lowest state S_1 (1.43 - 1.62 eV, RI =0.020 for 1.43 eV) of the experimental results matches nicely with the first peak of 1.46 eV (ROS = 0.051) obtained in the screened parameter calculations, than the corresponding one for the standard parameter case located at 1.82 eV. The second state of the experimental results, S_3 (2.33 eV, RI = 0.033) again agrees much better with the second peak of the screened parameter result, 2.45 eV (ROS = 0.043) than with the standard parameter one located at 2.79 eV. The third state of the experimental results, S_4 (2.50 eV, RI = 0.023) has a better agreement with the third state of the screened parameter spectrum 2.71 eV (ROS = 0.020) than with the corresponding standard parameter peak at 3.80 eV. The most intense peak in the experimental results is S_9 (3.66 eV, RI = 1.0) lies in between the highest peak of the screened and standard parameter calculations located at 3.32 eV (ROS = 1.0), and 3.80 eV (ROS = 1.0), respectively. For this most intense peak, the standard parameter results appear to agree slightly better with the experiments, as compared to the screened ones. But, keeping in mind the lower energy peaks discussed above, overall the screened parameter based results have a much better agreement with the experiments, just as in case of octacene. Similar to octacene, we again note that with the increasing peak energy, the agreement between the experiments and theory begins to deteriorate, which we again attribute to the reduced computational accuracy for higher energies. As far as the comparison of the experimental results with the triplet absorption calculations (cf., Ref.[39]) is concerned, the first peaks in the computed triplet spectra, 2.56 eV (ROS=0.785) for the standard parameter, and 1.86 eV (ROS=1.0) for the screened parameters, disagree completely with the location of S_1, as well as its relative intensity in the experimental spectrum. The same trend holds for the higher excited states as well. Thus, we conclude that the experimental absorption spectrum of nonacene is indeed from the $1^1A_g^-$ ground state of the system, confirming yet again that the ground state of nonacene has the singlet multiplicity. Again, we note that the DMRG based calculations employing the PPP model, performed by Raghu *et al.*[31] predict an unrealistically large optical gap of 2.59 eV for nonacene. Our values of the calculated optical gaps of octacene, nonacene, and decacene are in very good agreement with the estimated optical gap of polyacene 1.18 ± 0.06 eV, reported by Tönshoff and Bettinger.[13]

To conclude, the experimentalists are confident that the absorptions which they observed are all from the ground states of octacene and nonacene. Because, our singlet absorption spectra (as against the triplet absorption) computed using the screened parameters are in excellent agreement with those experiments, we conclude that the ground states of octacene and nonacene are of singlet multiplicity (1^1A_g), in perfect agreement with our singlet-triplet crossover calculations. Although the experiments have not been performed on acenes longer than nonacene, the trend emerging from our calculations leads us to conclude that the ground state will be of singlet type in those systems as well.

IV. CONCLUSIONS

To summarize, we presented large-scale MRSDCI calculations on the electronic structure and optical properties of oligoacenes, with focus on the longer acenes, namely, octacene, nonacene, and decacene. By performing such calculations on the lowest singlet and triplet states of oligomers ranging from naphthalene up to decacene, we established that the ground state in oligoacenes has singlet multiplicity, with a singlet-triplet gap of approximately 0.5 eV even for decacene. The trends visible from our calculations rule out a singlet-triplet crossover for the ground states of longer oligoacenes as well. This result of ours has thus resolved an old speculation predicting that nonacene onwards, the ground state of oligoacenes will be of triplet multiplicity.[15]

Moreover, the many-body wavefunction analysis of the correlated singlet ground state $1^1A_g^-$ reveals increasing contribution of configurations with two open shells, accompanied with the decreasing one from the closed-shell Hartree-Fock reference state, with the increasing chain length. Thus our calculations predict an open-shell diradical character for the singlet ground state of longer acenes.[28]

As far as the singlet linear optical absorption is concerned, in all the acenes, the first peak is due to a y-polarized transition to the $1^1B_{2u}^+$ state, corresponding to the HOMO to LUMO transition. The most intense state is the x-polarized transition to a $^1B_{3u}$ state, which is also dominated by single excitations. When we compare our singlet linear absorption spectra of octacene and nonacene with the experimental ones,[13] excellent agreement is obtained on the important peak locations and intensity profiles. Furthermore, the measured absorption spectra of longer acenes show no resemblance with our computed triplet absorption spectra, confirming once again the conclusion that the ground state of the longer acenes is indeed singlet in nature.

Our calculations on the one-photon triplet absorption spectra predict two intense x-polarized absorptions, which are well separated in energy. Besides these two, there are a number of weaker peaks which are either x or y polarized. This is in sharp contrast to the singlet absorption which predicts only one intense peak. The existence of two well separated x-polarized peaks in the triplet absorption spectrum is one of the most important predictions of this work, and can be tested in future experiments on oriented samples of longer acenes.

We also performed singlet and triplet optical absorption calculations on decacene, a molecule which has not been synthesized yet. We are hopeful that in future, once decacene is synthesized in the laboratory, our theoretical predictions could be tested in experiments.

In this paper we restricted ourselves to the low-lying excited states of longer acenes which contribute to their linear optical properties. However, not many calculations have been performed as far as the nonlinear optical properties of these materials are concerned. In particular, it will be of interest to compute the nonlinear susceptibilities corresponding to two-photon absorption, and third harmonic generation. Both these nonlinear optical processes have the capability to probe the higher excited states of polyacenes, which is essential in order to obtain a deeper understanding of the optical response of π electrons. At present, studies along these directions are underway in our group.

ACKNOWLEDGMENTS

The authors thank Professor H. F. Bettinger (University of Tübingen) for communicating his experimental data before publications. One of us (H. C.) acknowledges the Council of Scientific and Industrial Research, (CSIR), India for the financial support (SRF award No. 20-06/2009(i)EU-IV).

---

[*] chakraborty.himanshu@gmail.com, shukla@phy.iitb.ac.in

[1] E. Clar, *Polycyclic Hydrocarbons* (Academic Press, London, New York 1964), Vol. 1, 2; E. Clar, *The Aromatic Sextet*, (Wiley, London, 1972); A. Bjorseth, Ed. *Handbook of Polycyclic Aromatic Hydrocarbons*, (Dekker, New York, 1983); M. Cooke, A. J. Dennis, Eds. *Polynuclear Aromatic Hydrocarbons: A Decade of Progress* (Battelle Press, Columbus, 1988); R. G. Harvey, *Polycyclic Aromatic Hydrocarbons*, (Wiley-VCH, New York, 1997).

[2] Y. Geerts, G. Klärner, in *Electronic Materials, the Oligomer Approach*, edited by G. Wegner, K. Müllen (Wiley-VCH, Weinheim, Germany, 1998), p. 48.

[3] M. Bendikov, F. Wudl, D. F. Perepichka, *Chem. Rev.* **104**, 4891 (2004).

[4] J. E. Anthony, *Chem. Rev.* **106**, 5028 (2006).

[5] See, *e.g.*, E. Clar, F. John, *Ber. Dtsch. Chem. Ges. B* **63**, 2967 (1930); H. B. Klevens and J. R. Platt, *J. Chem. Phys.* **17**, 470 (1949).

[6] J. E. Anthony, *Angew. Chem. Int. Ed.* **47**, 452 (2008).

[7] D. Biermann and W. Schmidt, *J. Am. Chem. Soc.* **102**, 3163 (1980).

[8] R. Mondal, C. Tönshoff, D. Khon, D. C. Neckers, and H. F. Bettinger, *J. Am. Chem. Soc.* **131**, 14281 (2009).

[9] R. Mondal, B. K. Shah, and D. C. Neckers, *J. Am. Chem. Soc.* **128**, 9612 (2006).

[10] H. F. Bettinger, R. Mondal, and D. Neckers, *Chem. Commun.* **48**, 5209 (2007).

[11] D. Chun, Y. Cheng, and F. Wudl, *Angew. Chem. Int. Ed.* **47**, 8380 (2008).

[12] M. M. Payne, S. R. Parkin, and J. E. Anthony, *J. Am. Chem. Soc.* **127**, 8028 (2005) .

[13] C. Tönshoff and H. F. Bettinger, *Angew. Chem. Int. Ed.* **49**, 4125 (2010).

[14] I. Kaur, M. Jazdzyk, N. N. Stein, P. Prusevich, and G. P. Miller, *J. Am. Chem. Soc.* **132**, 1261 (2010).

[15] H. Angliker, E. Rommel, and J. Wirz, *Chem. Phys. Lett.* **87**, 208 (1982).

[16] P. Sony and A. Shukla, *Phys. Rev. B* **75**, 155208 (2007).

[17] P. Sony and A. Shukla, *J. Chem. Phys.* **131**, 014302 (2009).

[18] C. Raghu, Y. Anusooya Pati, and S. Ramasesha, *Phys. Rev. B* **65**, 155204 (2002).

[19] K. Ohno, *Theor. Chim. Acta* **2**, 219 (1964).

[20] M. Chandross and S. Mazumdar, *Phys. Rev. B* **55**, 1497 (1997).

[21] Sony, P.; Shukla, A. *Comp. Phys. Comm.* **2010**, *181*, 821.

[22] H. Ghosh, A. Shukla, and S. Mazumdar, *Phys. Rev. B* **62**, 12763 (2000).

[23] A. Shukla, *Phys. Rev. B* **65**, 125204 (2002).

[24] A. Shukla, *Chem. Phys.* **300**, 177 (2004).

[25] A. Shukla, *Phys. Rev. B* **69**, 165218 (2004).

[26] K.N. Houk, P.S. Lee, and M. Nendel, *J. Org. Chem.* **66**, 5517 (2001).

[27] See, e.g., D. Barieswyl, D. K. Campbell, and S. Mazumdar, in *Conjugated Conducting Polymers*, edited by H. Keiss (Springer-Verlag, Berlin, 1992), pp. 7-133.

[28] M. Bendikov, H. M. Duong, K. Starkey, K. N. Houk, E. A. Carter, and F. Wudl, *J. Am. Chem. Soc.* **126**, 7416 (2004); **126**, 10493 (E) (2004).

[29] J. Hachmann, J. J. Dorando, M. Avilés, and G. K.-L. Chan, *J. Chem. Phys.* **127**, 134309 (2007).

[30] B. Hajgató, M. Huzak, and M. S. Deleuze, *J. Phys. Chem. A* **115**, 9282 (2011).

[31] C. Raghu, Y. Anusooya Pati, and S. Ramasesha, *Phys. Rev. B* **66**, 035116 (2002).

[32] Y. Gao, C.-G. Liu, and Y.-S. Jiang, *J. Phys. Chem. A* **106**, 2592 (2002).

[33] L. Salem and C. Rowland, *Angew. Chem. Int. Ed.* **11**, 92 (1972).

[34] D. Jiang and S. Dai, *J. Phys. Chem. A* **112**, 332 (2008).

[35] J. B. Birks, *Photophysics of Aromatic Molecules* (Wiley-Interscience, New York, 1970).

[36] J. Schiedt and R. Weinkauf, *Chem. Phys. Lett.* **266,** 201 (1997).

[37] N. Sabbatini, M. T. Indelli, M. T. Gandolfi, and V. Balzani, *J. Phys. Chem.* **86,** 3585 (1982).

[38] J. Burgos, M. Pope, Ch. E. Swenberg, and R. R. Alfano, *Phys. Status Solidi B* **83**, 249 (1977).

[39] See EPAPS supplementary material for the tables.

[40] S. Rayne and K. Forest, *Nature Precedings* doi:10.1038/npre.2011.6578.1 (2011).

Supplementary Information: Detailed Description of Calculated Spectra

V. SINGLET LINEAR ABSORPTION

Here we present a detailed description of the calculated singlet linear absorption spectra of octacene, nonacene, and decacene, presented in Figures 4, 5 and 6 of the main text. Our calculations reveal the following features*:*

1. For all the oligoacene, the first peak is due to a y-polarized transition, to the $1^1B_{2u}^+$ excited state of the system, whose wave function is dominated by the $|H \rightarrow L\rangle$ single excitation, irrespective of the choice of the Coulomb parameters employed in the PPP model.

2. The second peak also corresponds to a y-polarized transition, to the $2^1B_{2u}^+$ excited state of the system. The most important configuration contributing to the many-particle wave function of this state is $|H-1 \rightarrow L+1\rangle$excitation, irrespective of the choice of the Coulomb parameters.

3. The nature of the third peak is dependent upon the Coulomb parameters employed in the PPP model. For the standard parameter case, this peak always corresponds to the x-polarized, $1^1B_{3u}^+$ excited state, signalling the onset of the most intense absorption feature in the system. For octacene, it is the single most intense peak, whose wave function mainly consists of single excitations $|H \rightarrow L+3\rangle + c.c.$ (*c.c.* denotes the charge conjugated configuration). For nonacene and decacene, perhaps due to band formation, it is the first of the two adjacent intense peaks which are x polarized. For nonacene it is the most intense peak, and the corresponding many-body wave function is dominated by the single excitation $|H \rightarrow L+4\rangle + c.c.$. For decacene, however, it is the second most intense feature, and the double excitations $|H \rightarrow L;\ H \rightarrow L+1\rangle + c.c.$ contribute the most to its many-body wave function.

   In the screened parameter calculations, the third peak is a faint peak, containing a mixture of x and y polarized transition to the states, $1^1B_{3u}^+$ and $3^1B_{2u}^+$ of the system. For all the oligoacenes, the double excitation $|H \rightarrow L;\ H \rightarrow L+1\rangle + c.c.$ contributes the most to the $1^1B_{3u}^+$ state, and the single excitation $|H \rightarrow L+2\rangle + c.c.$ dominates the $3^1B_{2u}^+$ wave function.

4. For the standard parameter case, the fourth peak is a faint peak for octacene, consisting of a mixture of x- and y-polarized transitions to the states, $2^1B_{3u}^+$ and $4^1B_{2u}^+$. Double excitations $|H \rightarrow L;\ H \rightarrow L+1\rangle + c.c.$ contribute the most to the $2^1B_{3u}^+$ state, and single excitations $|H-2 \rightarrow L+2\rangle + c.c.$ to the $4^1B_{2u}^+$ state. For nonacene and decacene, however, it is an intense x-polarized feature corresponding to the state $2^1B_{3u}^+$, which is adjacent to their $1^1B_{3u}^+$ state mentioned above. For the case of decacene, it also the most intense absorption of the system. Both for nonacene and decacene, the single excitations $|H \rightarrow L+4\rangle + c.c.$ contribute the most to the many-particle wave function of this state.

For the screened parameter calculations, the fourth peak corresponds to the most intense absorption, through an x-polarized photon, to the $2^1B_{3u}^+$ state, in case of octacene and nonacene. For decacene, however, it appears as a shoulder to the most intense peak, consisting of a mixture of x and y polarized transitions, to the $2^1B_{3u}^+$ and $4^1B_{2u}^+$ states. The many-particle wave function of the $2^1B_{3u}^+$ state for octacene and nonacene is dominated by the single excitations $|H \rightarrow L+4\rangle + c.c.$, while for decacene the double excitations $|H \rightarrow L+1;\, H \rightarrow L+2\rangle + c.c.$ dominate. The $4^1B_{2u}^+$ state of decacene has the maximum contribution from the single excitation $|H-2 \rightarrow L+2\rangle$.

5. For the standard parameter case, the fifth peak is a very faint feature consisting of y-polarized transition to the state $7^1B_{2u}^+$ for octacene, whose wave function is dominated by the single excitation $|H-2 \rightarrow L+2\rangle$. However, for nonacene and decacene, it corresponds to the mixture of x and y polarized transitions to the states, $3^1B_{3u}^+$ and $5^1B_{2u}^+$, respectively. The double excitations $|H \rightarrow L+1;\, H-1 \rightarrow L+1\rangle + c.c.$ for the $3^1B_{3u}^+$ state, and the triple excitation $|H \rightarrow L;\, H \rightarrow L;\, H-1 \rightarrow L+1\rangle$ for the $5^1B_{2u}^+$ state, contribute the most to their wave functions.

   For the screened parameter case, it is a faint peak consisting of a mixture of x and y polarized transitions to the states, $3^1B_{3u}^+$ and $4^1B_{2u}^+$, respectively, for both octacene and nonacene. For decacene, however, it is the most intense peak corresponding to x polarized transition to the state $4^1B_{3u}^+$. The most important configuration contributing to the many-particle wave function of the state for octacene and nonacene, is a mixture of double excitations $|H \rightarrow L+1;\, H \rightarrow L+2\rangle + c.c.$ for $3^1B_{3u}^+$ state, and single excitations $|H-2 \rightarrow L+2\rangle$ for the $4^1B_{2u}^+$ state. For decacene, the single excitations $|H \rightarrow L+5\rangle + c.c.$ contribute the most to the wavefunction of this state.

6. For the standard parameter case, the sixth peak corresponds to a mixture of x and y polarized transitions to the states, $4^1B_{3u}^+$ and $9^1B_{2u}^+$, respectively, for octacene. The many-body wave functions of both these states derive predominant contributions from double excitations: $|H \rightarrow L;\, H-1 \rightarrow L+2\rangle + c.c.$ for the $4^1B_{3u}^+$, and $|H \rightarrow L+1;\, H \rightarrow L+3\rangle + c.c.$ for the $9^1B_{2u}^+$ state. For nonacene (decacene), it corresponds to a y-polarized transition to the state $10^1B_{2u}^+$ ($9^1B_{2u}^+$), whose many-body wave function derives maximum contribution from the single excitation $|H-2 \rightarrow L+2\rangle$.

   The same peak with the screened parameters is a mixture of x and y polarized transitions for the case of octacene and nonacene. For octacene, transitions to states $6^1B_{3u}^+$ and $8^1B_{2u}^+$ constitute this peak, with double excitations $|H \rightarrow L;\, H \rightarrow L+1\rangle + c.c.$ and $|H \rightarrow L;\, H \rightarrow L+5\rangle + c.c.$, respectively, contributing most to their wave functions. For nonacene, this peak consists of three states $4^1B_{3u}^+$ and $6^1B_{2u}^+$ and $7^1B_{2u}^+$, with double excitation $|H \rightarrow L;\, H-1 \rightarrow L+2\rangle + c.c.$ contributing the most to the $4^1B_{3u}^+$, triple excitation $|H \rightarrow L;\, H \rightarrow L;\, H-1 \rightarrow L+1\rangle$ to the $6^1B_{2u}^+$, and the single excitation $|H-2 \rightarrow L+2\rangle$ to the $7^1B_{2u}^+$ state. However, for decacene, the peak is purely x polarized, due to transition to the state $6^1B_{3u}^+$ whose wave function derives maximum contribution from the double excitations $|H \rightarrow L;\, H \rightarrow L+1\rangle + c.c.$.

7. The seventh peak in the standard parameter spectrum is both x and y polarized for all the three oligomers. For octacene, the peak involves $5^1B_{3u}^+$ and $10^1B_{2u}^+$ states, with single excitations $|H \rightarrow L+7\rangle + c.c.$ and $|H-2 \rightarrow L+2\rangle$, respectively, contributing

the most to their wave functions. For nonacene states $7^1B_{3u}^+$ and $12^1B_{2u}^+$ constitute the peak, with single excitation $|H \rightarrow L+8\rangle$+c.c. providing the maximum contribution to the $7^1B_{3u}^+$ state, and triple excitation $|H \rightarrow L;\, H-1 \rightarrow L+1;\, H-1 \rightarrow L+1\rangle$ to the $12^1B_{2u}^+$ state. For decacene, the peak involves $6^1B_{3u}^+$ and $11^1B_{2u}^+$ states, with double excitations $|H \rightarrow L;\, H-1 \rightarrow L+2\rangle + c.c.$ and triple excitations $|H \rightarrow L;\, H-1 \rightarrow L+1;\, H-1 \rightarrow L+1\rangle$, respectively, contributing the most to their wave functions.

With the screened parameters, the seventh peak of octacene and nonacene is x polarized, while for decacene it has mixed x and y polarizations. Both for octacene and nonacene states $8^1B_{3u}^+$ constitute this peak, with single excitation $|H-1 \rightarrow L+5\rangle + c.c.$ and $|H-1 \rightarrow L+6\rangle + c.c.$ providing main contributions to the wave functions of octacene, and nonacene, respectively. However, for decacene, transitions to states $8^1B_{3u}^+$ and $10^1B_{2u}^+$ form the peak, with double excitations $|H \rightarrow L;\, H-1 \rightarrow L+4\rangle + c.c.$ and single excitations $|H-1 \rightarrow L+7\rangle + c.c.$, respectively, contributing the most to their wave functions.

8. With the standard parameters, the eighth peak does not exist for octacene, while for nonacene and decacene, it has mixed x and y polarizations. For nonacene, the states constituting the peak are $8^1B_{3u}^+$ and $16^1B_{2u}^+$, with single excitations $|H-1 \rightarrow L+5\rangle + c.c.$ and triple excitations $|H \rightarrow L;\, H \rightarrow L+2;\, H-1 \rightarrow L+1\rangle + c.c.$, respectively, contributing to their wave functions. For decacene, three states $7^1B_{3u}^+$, $14^1B_{2u}^+$, and $15^1B_{2u}^+$, form this peak, with single excitations $|H \rightarrow L+8\rangle + c.c.$, $|H \rightarrow L+12\rangle + c.c.$, and $|H \rightarrow L+9\rangle + c.c.$, respectively, contributing the most to their many-particle wave functions.

   With the screened parameters case, the eighth peak is x and y polarized for octacene and decacene, while it is only x polarized for nonacene. For octacene, states $9^1B_{3u}^+$ and $13^1B_{2u}^+$ form this peak, whose wave functions, respectively, derive maximum contributions from single excitations $|H-2 \rightarrow L+4\rangle + c.c.$, and triple excitations $|H \rightarrow L;\, H-1 \rightarrow L+1;\, H-1 \rightarrow L+1\rangle$. In case of nonacene, the transition to the state $9^1B_{3u}^+$ leads to this peak, with single excitations $|H-2 \rightarrow L+4\rangle + c.c.$ contributing the most to its many-particle wave function. For decacene, states $9^1B_{3u}^+$ and $14^1B_{2u}^+$ constitute the peak, with the single excitations $|H \rightarrow L+8\rangle + c.c.$ and $|H \rightarrow L+9\rangle + c.c.$, respectively, providing the largest contributions to their wave functions.

9. The ninth peak, for the standard parameter case, exists only for decacene, and has a mixed x and y polarization, with states $8^1B_{3u}^+$ and $17^1B_{2u}^+$ forming the peak. The single excitations $|H-2 \rightarrow L+4\rangle + c.c.$ contribute the most to $8^1B_{3u}^+$ state, while double excitations $|H \rightarrow L;\, H-1 \rightarrow L+4\rangle + c.c.$ to the $17^1B_{2u}^+$ state.

   With the screened parameters, the ninth peak does not exist for nonacene, and it is x and y polarized for octacene and decacene. For octacene, states $12^1B_{3u}^+$ and $16^1B_{2u}^+$ constitute this peak, with the double excitations $|H \rightarrow L;\, H-1 \rightarrow L+6\rangle + c.c.$ and single excitations $|H-1 \rightarrow L+7\rangle + c.c.$, respectively, contributing the most to their wave functions. For decacene, the states $11^1B_{3u}^+$ and $16^1B_{2u}^+$ form this peak, with the single excitations $|H-2 \rightarrow L+5\rangle + c.c.$ and $|H-1 \rightarrow L+7\rangle + c.c.$, respectively, providing the maximum contributions to their wave functions.

Table VI: Excited states contributing to the singlet linear absorption spectrum of octacene computed using the MRSDCI method coupled with the standard parameters in the PPP model Hamiltonian. The table includes many particle wave functions, excitation energies, dipole matrix elements, and relative oscillator strengths (ROS) of various states with respect to the 1^1A_g ground state. DF corresponds to dipole forbidden state. Below, '$+c.c.$' indicates that the coefficient of charge conjugate of a given configuration has the same sign, while '$-c.c.$' implies that the two coefficients have opposite signs.

Peak	State	E (eV)	Transition Dipole (Å)	ROS	Wave Functions
DF	$1^1B_{3u}^-$	2.31	0	0	$\vert H \rightarrow L; H \rightarrow L+1 \rangle - c.c.(0.4948)$ $\vert H \rightarrow L; H-1 \rightarrow L+2 \rangle - c.c.(0.1938)$
I	$1^1B_{2u}^+$	2.24	0.905	0.034	$\vert H \rightarrow L \rangle\ (-0.8471)$ $\vert H \rightarrow L; H \rightarrow L; H-1 \rightarrow L+1 \rangle\ (0.0948)$
II	$2^1B_{2u}^+$	3.34	0.641	0.025	$\vert H-1 \rightarrow L+1 \rangle\ (-0.5826)$ $\vert H \rightarrow L+2 \rangle - c.c.(0.4284)$
III	$1^1B_{3u}^+$	4.17	3.622	1.000	$\vert H \rightarrow L+3 \rangle + c.c.(0.4622)$ $\vert H \rightarrow L; H \rightarrow L+1 \rangle + c.c.(0.2614)$
IV	$4^1B_{2u}^+$	4.51	0.367	0.011	$\vert H-2 \rightarrow L+2 \rangle\ (-0.4148)$ $\vert H-1 \rightarrow L+4 \rangle + c.c.(0.4020)$
	$2^1B_{3u}^+$	4.57	1.079	0.097	$\vert H \rightarrow L; H \rightarrow L+1 \rangle + c.c.(0.3214)$ $\vert H \rightarrow L+3 \rangle + c.c.(0.3214)$
V	$7^1B_{2u}^+$	5.46	0.375	0.014	$\vert H-2 \rightarrow L+2 \rangle\ (0.3574)$ $\vert H \rightarrow L+6 \rangle - c.c.(0.3489)$
VI	$9^1B_{2u}^+$	5.64	0.261	0.007	$\vert H \rightarrow L+1; H \rightarrow L+3 \rangle + c.c.(0.3883)$ $\vert H \rightarrow L; H \rightarrow L+5 \rangle + c.c.(0.2768)$
	$4^1B_{3u}^+$	5.65	0.335	0.012	$\vert H \rightarrow L; H-1 \rightarrow L+2 \rangle - c.c.(0.4696)$ $\vert H \rightarrow L; H \rightarrow L+1 \rangle + c.c.(0.1289)$
VII	$10^1B_{2u}^+$	5.89	0.203	0.004	$\vert H-2 \rightarrow L+2 \rangle\ (-0.3657)$ $\vert H-3 \rightarrow L+3 \rangle\ (0.3074)$
	$5^1B_{3u}^+$	5.94	0.307	0.010	$\vert H \rightarrow L+7 \rangle - c.c.(0.3397)$ $\vert H \rightarrow L; H \rightarrow L+4 \rangle + c.c.(0.2494)$

Table VII: Excited states contributing to the singlet linear absorption spectrum of octacene computed using the MRSDCI method coupled with the screened parameters in the PPP model Hamiltonian. The rest of the information is same as that in VI.

Peak	State	E (eV)	Transition Dipole (Å)	ROS	Wave Functions
DF	$1^1B_{3u}^-$	1.59	0	0	$\|H \rightarrow L; H \rightarrow L+1\rangle - c.c.(0.5078)$ $\|H \rightarrow L; H-1 \rightarrow L+2\rangle - c.c.(0.1949)$
I	$1^1B_{2u}^+$	1.49	1.241	0.050	$\|H \rightarrow L\rangle\ (0.8503)$ $\|H \rightarrow L; H \rightarrow L; H-1 \rightarrow L+1\rangle\ (0.0929)$
II	$2^1B_{2u}^+$	2.65	0.897	0.047	$\|H-1 \rightarrow L+1\rangle\ (-0.7244)$ $\|H \rightarrow L+2\rangle + c.c.(0.2638)$
III	$3^1B_{2u}^+$	2.89	0.440	0.012	$\|H \rightarrow L+2\rangle + c.c.(0.5326)$ $\|H-1 \rightarrow L+1\rangle\ (-0.3290)$
	$1^1B_{3u}^+$	2.97	0.845	0.046	$\|H \rightarrow L; H \rightarrow L+1\rangle - c.c.(0.4942)$ $\|H \rightarrow L+1; H-1 \rightarrow L+1\rangle - c.c.(0.2522)$
IV	$2^1B_{3u}^+$	3.38	3.675	1.000	$\|H \rightarrow L+4\rangle + c.c.(0.5831)$ $\|H-1 \rightarrow L+5\rangle + c.c.(0.1004)$
V	$3^1B_{3u}^+$	3.91	0.410	0.014	$\|H \rightarrow L+1; H \rightarrow L+2\rangle - c.c.(0.4028)$ $\|H \rightarrow L+1; H \rightarrow L+4\rangle - c.c.(0.3003)$
	$4^1B_{2u}^+$	3.97	0.641	0.036	$\|H-2 \rightarrow L+2\rangle\ (-0.5280)$ $\|H-1 \rightarrow L+3\rangle + c.c.(0.3722)$
VI	$8^1B_{2u}^+$	4.52	0.230	0.005	$\|H \rightarrow L; H \rightarrow L+5\rangle - c.c.(0.4706)$ $\|H \rightarrow L; H-1 \rightarrow L+4\rangle - c.c.(0.3075)$
	$6^1B_{3u}^+$	4.57	0.403	0.016	$\|H \rightarrow L; H \rightarrow L+1\rangle - c.c.(0.3419)$ $\|H \rightarrow L; H \rightarrow L+3\rangle - c.c.(0.2890)$
VII	$8^1B_{3u}^+$	4.80	1.301	0.178	$\|H-1 \rightarrow L+5\rangle + c.c.(0.5537)$ $\|H \rightarrow L; H-1 \rightarrow L+2\rangle - c.c.(0.1321)$
VIII	$9^1B_{3u}^+$	5.14	0.410	0.019	$\|H-2 \rightarrow L+4\rangle + c.c.(0.5720)$ $\|H \rightarrow L+2; H \rightarrow L+3\rangle - c.c.(0.0943)$
	$13^1B_{2u}^+$	5.22	0.418	0.020	$\|H \rightarrow L; H-1 \rightarrow L+1; H-1 \rightarrow L+1\rangle\ (0.3505)$ $\|H-1 \rightarrow L+7\rangle + c.c.(0.2709)$
IX	$16^1B_{2u}^+$	5.53	0.440	0.023	$\|H-1 \rightarrow L+7\rangle + c.c.(0.3983)$ $\|H-3 \rightarrow L+3\rangle\ (0.3636)$
	$12^1B_{3u}^+$	5.66	0.154	0.003	$\|H \rightarrow L; H-1 \rightarrow L+6\rangle - c.c.(0.4014)$ $\|H \rightarrow L+2; H-2 \rightarrow L+1\rangle - c.c.(0.3019)$

Table VIII: Excited states contributing to the singlet linear absorption spectrum of nonacene computed using the MRS-DCI method coupled with the standard parameters in the PPP model Hamiltonian. The rest of the information is same as that in VI.

Peak	State	E (eV)	Transition Dipole (Å)	ROS	Wave Functions
DF	$1^1B_{3u}^-$	1.86	0	0	$\|H \rightarrow L; H \rightarrow L+1\rangle + c.c.(0.4872)$ $\|H \rightarrow L+1; H \rightarrow L+2\rangle + c.c.(0.2027)$
I	$1^1B_{2u}^+$	1.82	1.328	0.092	$\|H \rightarrow L\rangle\ (0.8290)$ $\|H \rightarrow L; H \rightarrow L; H-1 \rightarrow L+1\rangle\ (0.1066)$

II	$2^1B_{2u}^+$	2.79	0.733	0.043	$\lvert H-1\rightarrow L+1\rangle$ (0.5506) $\lvert H\rightarrow L+2\rangle + c.c.(0.4342)$
III	$1^1B_{3u}^+$	3.80	3.037	1.000	$\lvert H\rightarrow L+4\rangle - c.c.(0.3757)$ $\lvert H\rightarrow L; H\rightarrow L+1\rangle - c.c.(0.3274)$
IV	$2^1B_{3u}^+$	4.12	2.583	0.786	$\lvert H\rightarrow L+4\rangle - c.c.(0.3943)$ $\lvert H\rightarrow L; H\rightarrow L+1\rangle - c.c.(0.2791)$
V	$5^1B_{2u}^+$	4.62	0.439	0.025	$\lvert H\rightarrow L; H\rightarrow L; H-1\rightarrow L+1\rangle$ (0.6215) $\lvert H-1\rightarrow L+1\rangle$ (0.2357)
	$3^1B_{3u}^+$	4.63	0.549	0.040	$\lvert H\rightarrow L+1; H-1\rightarrow L+1\rangle - c.c.(0.3339)$ $\lvert H\rightarrow L+1; H\rightarrow L+2\rangle - c.c.(0.3035)$
VI	$10^1B_{2u}^+$	5.29	0.457	0.032	$\lvert H-2\rightarrow L+2\rangle$ (−0.3824) $\lvert H\rightarrow L+1; H\rightarrow L+4\rangle + c.c.(0.2681)$
VII	$7^1B_{3u}^+$	5.71	0.277	0.013	$\lvert H\rightarrow L+8\rangle - c.c.(0.3021)$ $\lvert H\rightarrow L; H\rightarrow L+3\rangle + c.c.(0.2619)$
	$12^1B_{2u}^+$	5.72	0.318	0.017	$\lvert H\rightarrow L; H-1\rightarrow L+1; H-1\rightarrow L+1\rangle$ (−0.3293) $\lvert H\rightarrow L; H-1\rightarrow L+4\rangle - c.c.(0.2869)$
VIII	$16^1B_{2u}^+$	5.94	0.287	0.014	$\lvert H\rightarrow L; H\rightarrow L+2; H-1\rightarrow L+1\rangle - c.c.(0.3742)$ $\lvert H\rightarrow L; H-1\rightarrow L+4\rangle - c.c.(0.2500)$
	$8^1B_{3u}^+$	5.95	0.996	0.169	$\lvert H-1\rightarrow L+5\rangle - c.c.(0.3932)$ $\lvert H-2\rightarrow L+4\rangle - c.c.(0.2993)$

Table IX: Excited states contributing to the singlet linear absorption spectrum of nonacene computed using the MRSDCI method coupled with the screened parameters in the PPP model Hamiltonian. The rest of the information is same as that in VI.

Peak	State	E (eV)	Transition Dipole (Å)	ROS	Wave Functions
DF	$1^1B_{3u}^-$	1.51	0	0	$\lvert H\rightarrow L; H\rightarrow L+1\rangle + c.c.(0.5143)$ $\lvert H\rightarrow L; H-1\rightarrow L+2\rangle - c.c.(0.2089)$
I	$1^1B_{2u}^+$	1.46	1.316	0.051	$\lvert H\rightarrow L\rangle$ (0.8551) $\lvert H\rightarrow L; H\rightarrow L; H-1\rightarrow L+1\rangle$ (0.1017)
II	$2^1B_{2u}^+$	2.45	0.935	0.043	$\lvert H-1\rightarrow L+1\rangle$ (0.7260) $\lvert H\rightarrow L+2\rangle - c.c.(0.2689)$
III	$1^1B_{3u}^+$	2.71	0.611	0.020	$\lvert H\rightarrow L; H\rightarrow L+1\rangle - c.c.(0.4901)$ $\lvert H\rightarrow L+1; H-1\rightarrow L+1\rangle - c.c.(0.2454)$
	$3^1B_{2u}^+$	2.77	0.507	0.014	$\lvert H\rightarrow L+2\rangle - c.c.(0.5434)$ $\lvert H-1\rightarrow L+1\rangle$ (−0.3462)
IV	$2^1B_{3u}^+$	3.32	3.887	1.000	$\lvert H\rightarrow L+4\rangle - c.c.(0.5689)$ $\lvert H-1\rightarrow L+6\rangle + c.c.(0.1185)$
V	$3^1B_{3u}^+$	3.63	0.782	0.044	$\lvert H\rightarrow L+1; H\rightarrow L+2\rangle + c.c.(0.3441)$ $\lvert H-1\rightarrow L+1; H\rightarrow L+1\rangle - c.c.(0.3221)$
	$4^1B_{2u}^+$	3.69	0.559	0.023	$\lvert H-2\rightarrow L+2\rangle$ (−0.4715) $\lvert H-1\rightarrow L+3\rangle + c.c.(0.4395)$

VI	$4^1B_{3u}^+$	3.93	0.369	0.011	$\vert H \rightarrow L; H-1 \rightarrow L+2 \rangle - c.c.(0.4953)$ $\vert H \rightarrow L; H \rightarrow L+3 \rangle - c.c.(0.2163)$
	$6^1B_{2u}^+$	4.01	0.690	0.038	$\vert H \rightarrow L; H \rightarrow L; H-1 \rightarrow L+1 \rangle\ (0.5954)$ $\vert H \rightarrow L+5 \rangle + c.c.(0.3166)$
	$7^1B_{2u}^+$	4.12	0.692	0.039	$\vert H-2 \rightarrow L+2 \rangle\ (-0.5949)$ $\vert H-1 \rightarrow L+3 \rangle + c.c.(0.3994)$
VII	$8^1B_{3u}^+$	4.61	1.450	0.193	$\vert H-1 \rightarrow L+6 \rangle + c.c.(0.5262)$ $\vert H \rightarrow L; H-1 \rightarrow L+2 \rangle - c.c.(0.1473)$
VIII	$9^1B_{3u}^+$	4.97	0.338	0.011	$\vert H-2 \rightarrow L+4 \rangle + c.c.(0.5823)$ $\vert H \rightarrow L+8 \rangle + c.c.(0.0699)$

Table X: Excited states contributing to the singlet linear absorption spectrum of decacene computed using the MRSDCI method coupled with the standard parameters in the PPP model Hamiltonian. The rest of the information is same as that in VI.

Peak	State	E (eV)	Transition Dipole (Å)	ROS	Wave Functions
DF	$1^1B_{3u}^-$	1.72	0	0	$\vert H \rightarrow L; H \rightarrow L+1 \rangle - c.c.(0.4790)$ $\vert H \rightarrow L+1; H \rightarrow L+2 \rangle + c.c.(0.2119)$
I	$1^1B_{2u}^+$	1.79	1.423	0.084	$\vert H \rightarrow L \rangle\ (-0.8203)$ $\vert H-1 \rightarrow L+1 \rangle\ (-0.1213)$
II	$2^1B_{2u}^+$	2.64	0.776	0.037	$\vert H-1 \rightarrow L+1 \rangle\ (-0.5607)$ $\vert H \rightarrow L+2 \rangle - c.c.(0.4239)$
III	$1^1B_{3u}^+$	3.68	2.554	0.553	$\vert H \rightarrow L; H \rightarrow L+1 \rangle + c.c.(0.3710)$ $\vert H \rightarrow L+4 \rangle + c.c.(0.2865)$
IV	$2^1B_{3u}^+$	4.00	3.293	1.000	$\vert H \rightarrow L+4 \rangle + c.c.(0.4451)$ $\vert H \rightarrow L+1; H \rightarrow L+2 \rangle - c.c.(0.2322)$
V	$5^1B_{2u}^+$	4.40	0.505	0.026	$\vert H \rightarrow L; H \rightarrow L; H-1 \rightarrow L+1 \rangle\ (-0.6203)$ $\vert H-1 \rightarrow L+1 \rangle\ (-0.2380)$
	$3^1B_{3u}^+$	4.46	0.739	0.056	$\vert H \rightarrow L+1; H-1 \rightarrow L+1 \rangle + c.c.(0.3459)$ $\vert H \rightarrow L+1; H \rightarrow L+2 \rangle - c.c.(0.2800)$
VI	$9^1B_{2u}^+$	5.05	0.392	0.018	$\vert H-2 \rightarrow L+2 \rangle\ (-0.3901)$ $\vert H-1 \rightarrow L+3 \rangle\ (-0.2482)$
VII	$6^1B_{3u}^+$	5.45	0.337	0.014	$\vert H \rightarrow L; H-1 \rightarrow L+2 \rangle - c.c.(0.3992)$ $\vert H \rightarrow L+8 \rangle - c.c.(0.2341)$
	$11^1B_{2u}^+$	5.45	0.351	0.015	$\vert H \rightarrow L; H-1 \rightarrow L+1; H-1 \rightarrow L+1 \rangle\ (-0.4912)$ $\vert H \rightarrow L; H \rightarrow L; H-1 \rightarrow L+1 \rangle\ (-0.2510)$
VIII	$7^1B_{3u}^+$	5.59	0.584	0.044	$\vert H \rightarrow L+8 \rangle\ (0.3796)$ $\vert H-1 \rightarrow L+6 \rangle - c.c.(0.2866)$
	$14^1B_{2u}^+$	5.62	0.332	0.014	$\vert H \rightarrow L+12 \rangle + c.c.(0.4160)$ $\vert H-1 \rightarrow L+7 \rangle + c.c.(0.2309)$
	$15^1B_{2u}^+$	5.63	0.326	0.014	$\vert H \rightarrow L+9 \rangle + c.c.(0.3036)$ $\vert H-1 \rightarrow L+7 \rangle + c.c.(0.2945)$

IX	$8^1B_{3u}^+$	5.89	0.913	0.113	$\vert H-2\rightarrow L+4\rangle - c.c.(0.3596)$ $\vert H-1\rightarrow L+6\rangle - c.c.(0.2949)$
	$17^1B_{2u}^+$	5.89	0.149	0.003	$\vert H\rightarrow L; H-1\rightarrow L+4\rangle - c.c.(0.4687)$ $\vert H\rightarrow L; H\rightarrow L; H-2\rightarrow L+2\rangle\ (-0.1847)$

Table XI: Excited states contributing to the singlet linear absorption spectrum of decacene computed using the MRSDCI method coupled with the screened parameters in the PPP model Hamiltonian. The rest of the information is same as that in VI.

Peak	State	E (eV)	Transition Dipole (Å)	ROS	Wave Functions
DF	$1^1B_{3u}^-$	1.15	0	0	$\vert H\rightarrow L; H\rightarrow L+1\rangle - c.c.(0.4851)$ $\vert H\rightarrow L+1; H-1\rightarrow L+2\rangle - c.c.(0.2102)$
I	$1^1B_{2u}^+$	1.27	1.369	0.067	$\vert H\rightarrow L\rangle\ (-0.8338)$ $\vert H\rightarrow L; H\rightarrow L; H-1\rightarrow L+1\rangle\ (+0.1112)$
II	$2^1B_{2u}^+$	2.16	0.929	0.052	$\vert H-1\rightarrow L+1\rangle\ (+0.7110)$ $\vert H\rightarrow L+2\rangle + c.c.(0.2625)$
III	$3^1B_{2u}^+$	2.42	0.417	0.012	$\vert H\rightarrow L+2\rangle + c.c.(0.5220)$ $\vert H-1\rightarrow L+1\rangle\ (-0.3185)$
	$1^1B_{3u}^+$	2.42	0.295	0.006	$\vert H\rightarrow L; H\rightarrow L+1\rangle + c.c.(0.4762)$ $\vert H-1\rightarrow L; H-1\rightarrow L+1\rangle + c.c.(0.2590)$
IV	$2^1B_{3u}^+$	3.20	1.872	0.315	$\vert H\rightarrow L+1; H\rightarrow L+2\rangle + c.c.(0.3455)$ $\vert H\rightarrow L+5\rangle + c.c.(0.2733)$
	$4^1B_{2u}^+$	3.21	0.706	0.045	$\vert H-2\rightarrow L+2\rangle\ (0.5140)$ $\vert H-1\rightarrow L+3\rangle + c.c.(0.3975)$
V	$4^1B_{3u}^+$	3.35	3.259	1.000	$\vert H\rightarrow L+5\rangle + c.c.(0.4970)$ $\vert H\rightarrow L; H-1\rightarrow L+2\rangle - c.c.(0.2002)$
VI	$6^1B_{3u}^+$	3.81	0.273	0.008	$\vert H\rightarrow L; H\rightarrow L+1\rangle - c.c.(0.3703)$ $\vert H\rightarrow L; H\rightarrow L+3\rangle + c.c.(0.3689)$
VII	$8^1B_{3u}^+$	4.32	0.184	0.004	$\vert H\rightarrow L; H-1\rightarrow L+4\rangle - c.c.(0.2891)$ $\vert H\rightarrow L+6; H-5\rightarrow L+2\rangle - c.c.(0.2750)$
	$10^1B_{2u}^+$	4.33	0.478	0.028	$\vert H-1\rightarrow L+7\rangle - c.c.(0.2951)$ $\vert H-2\rightarrow L+4\rangle - c.c.(0.2793)$
VIII	$9^1B_{3u}^+$	4.51	0.330	0.014	$\vert H\rightarrow L+8\rangle + c.c.(0.4467)$ $\vert H\rightarrow L+2; H-1\rightarrow L+2\rangle + c.c.(0.2155)$
	$14^1B_{2u}^+$	4.56	0.376	0.018	$\vert H\rightarrow L+9\rangle + c.c.(0.4944)$ $\vert H-3\rightarrow L+7\rangle\ (-0.2478)$
IX	$11^1B_{3u}^+$	4.77	0.754	0.076	$\vert H-2\rightarrow L+5\rangle + c.c.(0.5543)$ $\vert H\rightarrow L+3; H-1\rightarrow L+1\rangle - c.c.(0.2076)$
	$16^1B_{2u}^+$	4.77	0.520	0.036	$\vert H-1\rightarrow L+7\rangle - c.c.(0.3795)$ $\vert H-3\rightarrow L+7\rangle\ (0.3359)$

VI. TRIPLET ABSORPTION

In the following we present a detailed description of the calculated triplet absorption spectra of octacene, nonacene, and decacene, presented in Figures 8, 9 and 10 of the main text.

1. The first peak always corresponds to the $1^3B_{1g}^-$ excited state of the system, whose wave function is dominated by the single excitations $|H \rightarrow L+1\rangle + c.c.$, irrespective of the oligoacene in question, or the Coulomb parameters employed.

2. The second peak corresponds to a y-polarized transition to the $1^3A_g^-$ excited state, for all the oligoacenes, irrespective of the Coulomb parameters employed. The most important configuration contributing to the many-particle wave function of the $1^3A_g^-$ state, is the double excitation $|H \rightarrow L;\ H-1 \rightarrow L+1\rangle$.

3. The nature of the third peak is dependent upon the Coulomb parameters employed in the PPP model. For the standard parameter case, this peak corresponds to a mixture of x- and y-polarized the transitions to states, $2^3B_{1g}^-$ and $3^3A_g^-$ for octacene and nonacene. For octacene, the single excitations $|H \rightarrow L+4\rangle + c.c.$ for the $2^3B_{1g}^-$ state, and $|H-1 \rightarrow L+3\rangle + c.c.$ for $3^3A_g^-$ state contribute the most to the respective wave functions. For nonacene, the single excitations $|H \rightarrow L+3\rangle + c.c.$ for the $2^3B_{1g}^-$ state, and the double excitation $|H \rightarrow L;\ H-1 \rightarrow L+1\rangle$ for the $3^3A_g^-$ states dominate the corresponding wave functions. However, for decacene, the peak corresponds to an x polarized transition to the state $2^3B_{1g}^-$, whose wave function is dominated by single excitations, with the configurations $|H \rightarrow L+3\rangle + c.c.$ contributing the most.

   For the screened parameter case, for all the oligomers, the third peak is due to an x-polarized transition to the state $3^3B_{1g}^-$ whose wave function derives the maximum contribution from the single excitations $|H \rightarrow L+3\rangle + c.c.$.

4. As far as the fourth peak is concerned, with standard parameters it corresponds to an x-polarized transition to the $3^3B_{1g}^-$ excited state, for all the oligoacenes. For octacene, it happens to be the most intense peak of the spectrum, but for nonacene and decacene, it is a shoulder to the most intense peak. Double excitations $|H \rightarrow L;\ H \rightarrow L+3\rangle + c.c.$ contribute the most to the many-particle wave function of this state for octacene, whereas for nonacene and decacene, the single excitations $|H-1 \rightarrow L+2\rangle + c.c.$ dominate the wave function.

   In the screened parameter spectrum, the fourth peak is due to a y-polarized transiton to the $3^3A_g^-$ state for octacene and nonacene. For octacene, the single excitations $|H \rightarrow L+5\rangle + c.c.$ contribute the most to the many particle wave function of this state, while for nonacene, the single excitations $|H \rightarrow L+6\rangle + c.c.$ dominate the state. However, for decacene, the fourth peak is the second most intense peak of the spectrum, corresponding to an x-polarized transition to the $6^3B_{1g}^-$ state, whose wave function is dominated by the double excitations $|H \rightarrow L;\ H \rightarrow L+5\rangle + c.c.$.

5. For the standard parameter case, the fifth peak is due to an x-polarized transition to the state $4^3B_{1g}^-$ for all the oligoacenes. For the case of octacene, it appears as a shoulder of the most intense peak (peak IV), while for nonacene and decacene it is the

most intense peak. For octacene the wave function of this state is composed mainly of single excitations, with configurations $|H-1 \rightarrow L+2\rangle + c.c.$ contributing the most. For nonacene and decacene, however, the wave function is dominated by the double excitations $|H \rightarrow L;\ H \rightarrow L+4\rangle + c.c.$.

In the screened parameter spectrum also the fifth peak corresponds to an x polarized transition for all the oligomers. For octacene, nonacene, and decacene, the states involved are $4^3B_{1g}^-$, $6^3B_{1g}^-$, and $8^3B_{1g}^-$, respectively. For octacene and nonacene, this peak is the second most intense one of the corresponding spectra, and the most important configuration contributing to the many-particle wave function of the states are the double excitations $|H \rightarrow L;\ H \rightarrow L+4\rangle + c.c.$. However, for decacene, it is a relatively weaker feature, with the double excitations $|H-1 \rightarrow L;\ H \rightarrow L+6\rangle + c.c.$ dominating the wave function of the state.

6. The sixth peak in the standard parameter spectrum, is formed by a y-polarized transition to the state $9^3A_g^-$ for the case of octacene, whose wave function is dominated by the single excitations $|H \rightarrow L+5\rangle + c.c.$ and $|H-3 \rightarrow L+1\rangle + c.c.$ However, for nonacene and decacene, it corresponds to an x-polarized transition to the state $6^3B_{1g}^-$, whose wave function receives maximum contribution from the triple excitations $|H \rightarrow L+1;\ H \rightarrow L+1;\ H-1 \rightarrow L\rangle + c.c.$.

   With the screened parameters, this peak is formed by an x-polarized transition to the state $7^3B_{1g}^-$ for octacene, with double excitations $|H \rightarrow L+1;\ H-5 \rightarrow L\rangle + c.c.$ dominating its wave function. For nonacene and decacene, the peak is due to mixed x and y polarized transitions. For nonacene, states $8^3B_{1g}^-$ and $10^3A_g^-$ form this peak, with their wave functions dominated by double excitations $|H \rightarrow L+1;\ H-6 \rightarrow L+1\rangle + c.c.$, and $|H-1 \rightarrow L+1;\ H \rightarrow L+2\rangle + c.c.$, respectively. For decacene, the states involved are $11^3B_{1g}^-$ and $14^3A_g^-$, with their wave functions dominated by the double excitations $|H \rightarrow L+1;\ H-1 \rightarrow L+5\rangle + c.c.$, and single excitations $|H-1 \rightarrow L+8\rangle + c.c.$, respectively.

7. With the the standard parameters, peak VII for octacene corrresponds to an x-polarized transition to the state $7^3B_{1g}^-$ with the double excitations $|H \rightarrow L;\ H-2 \rightarrow L+3\rangle + c.c.$ dominating its wave function. However, for nonacene and decacene this peak corresponds to a mixed x- and y-polarized transition. For nonacene, the states involved are $7^3B_{1g}^-$ and $11^3A_g^-$, with the double excitations $|H \rightarrow L+1;\ H-5 \rightarrow L\rangle + c.c.$, and single excitations $|H \rightarrow L+5\rangle + c.c.$, contributing the most to their respective wave functions. For decacene, the states forming the peak are $8^3B_{1g}^-$ and $11^3A_g^-$, of which the former is dominated by the double and triple excitations, while the latter consists mainly of the single excitations.

   Screened parameter calculations predict peak VII to have a mixed x and y polarized character for all the oligomers. For the case of octacene, four states $11^3B_{1g}^-$, $12^3B_{1g}^-$, $11^3A_g^-$, and $12^3A_g^-$, form this peak and the double excitations dominate the wave function of the first three states, while $12^3A_g^-$ is dominated by the single excitations. For nonacene, two states $11^3B_{1g}^-$ and $12^3A_g^-$ shape the peak with the triple excitations ($|H \rightarrow L;\ H \rightarrow L;\ H-1 \rightarrow L+2\rangle + c.c.$) dominating the wave function of the former, and single excitations ($|H-1 \rightarrow L+8\rangle + c.c.$) that of the latter. For decacene, three states, $13^3B_{1g}^-$, $14^3B_{1g}^-$, and $15^3A_g^-$, contribute to the peak, with the double excitations dominating all their wave functions.

8. In the standard parameter spectrum, peak VIII has a mixed x and y polarized character for octacene, but only a y-polarized character for nonacene and decacene. For octacene, the peak is formed by states $8^3B_{1g}^-$ and $12^3A_g^-$, of which the wave function of the former is dominated by the triple and double excitations, while that of the latter by double and single excitations. For nonacene, the state in question is $13^3A_g^-$, while for decacene it is $12^3A_g^-$, and wave functions in both the cases are dominated by doubly-excited configurations.

   In the screened parameter calculations, peak VIII exists only for octacene and nonacene, and is due to an x-polarized transition. For octacene it is formed by the state $13^3B_{1g}^-$, whose wave function is dominated by both single and double excitations. For nonacene, the peak is caused by the state $12^3B_{1g}^-$, whose wave function mainly consists of double excitations.

Table XII: Excited states contributing to the triplet absorption spectrum of octacene computed using the MRSDCI method coupled with the standard parameters in the PPP model Hamiltonian. The table includes many-particle wave functions, excitation energies, dipole matrix elements, and relative oscillator strengths (ROS) of various states. The excitation energies are with respect to the $1^1A_g^-$, ground state, while the dipole matrix elements, and the ROS, are with respect to the $1^3B_{2u}^+$ state. Below, '+*c.c.*' indicates that the coefficient of charge conjugate of a given configuration has the same sign, while '−*c.c.*' implies that the two coefficients have opposite signs.

Peak	State	E (eV)	Transition Dipole (Å)	ROS	Wave Functions
I	$1^3B_{1g}^-$	3.04	2.950	0.839	$\lvert H \rightarrow L+1\rangle - c.c.(0.5638)$ $\lvert H-1 \rightarrow L+2\rangle + c.c.(0.1836)$
II	$1^3A_g^-$	3.89	0.997	0.123	$\lvert H \rightarrow L; H-1 \rightarrow L+1\rangle$ (0.8187) $\lvert H \rightarrow L; H-2 \rightarrow L+2\rangle$ (0.1135)
III	$3^3A_g^-$	4.28	0.355	0.017	$\lvert H-1 \rightarrow L+3\rangle - c.c.(0.3698)$ $\lvert H \rightarrow L+5\rangle - c.c.(0.3435)$
	$2^3B_{1g}^-$	4.35	0.579	0.046	$\lvert H \rightarrow L+4\rangle - c.c.(0.5362)$ $\lvert H-1 \rightarrow L+2\rangle + c.c.(0.1999)$
IV	$3^3B_{1g}^-$	5.06	2.494	1.000	$\lvert H \rightarrow L; H \rightarrow L+3\rangle - c.c.(0.4566)$ $\lvert H-1 \rightarrow L+2\rangle + c.c.(0.3011)$
V	$4^3B_{1g}^-$	5.26	1.199	0.240	$\lvert H-1 \rightarrow L+2\rangle + c.c.(0.3688)$ $\lvert H \rightarrow L; H \rightarrow L+3\rangle - c.c.(0.2757)$
VI	$9^3A_g^-$	5.82	0.588	0.064	$\lvert H \rightarrow L+5\rangle - c.c.(0.3967)$ $\lvert H-3 \rightarrow L+1\rangle - c.c.(0.3809)$

VII	$7^3B_{1g}^-$	6.10	1.055	0.216	$\lvert H \rightarrow L; H-2 \rightarrow L+3 \rangle - c.c.(0.4326)$ $\lvert H \rightarrow L+1; H-1 \rightarrow L+3 \rangle - c.c.(0.1274)$
VIII	$8^3B_{1g}^-$	6.29	0.864	0.149	$\lvert H \rightarrow L+1; H \rightarrow L+1; H-1 \rightarrow L \rangle - c.c.(0.4030)$ $\lvert H \rightarrow L; H-2 \rightarrow L+3 \rangle - c.c.(0.3504)$
	$12^3A_g^-$	6.29	0.149	0.004	$\lvert H-1 \rightarrow L+1; H \rightarrow L+2 \rangle - c.c.(0.3707)$ $\lvert H-3 \rightarrow L+4 \rangle - c.c.(0.2968)$

Table XIII: Excited states contributing to the triplet absorption spectrum of octacene computed using the MRSDCI method coupled with the screened parameters in the PPP model Hamiltonian. The rest of the information is same as that in XII.

Peak	State	E (eV)	Transition Dipole (Å)	ROS	Wave Functions
I	$1^3B_{1g}^-$	1.97	4.639	1.000	$\lvert H \rightarrow L+1 \rangle + c.c.(0.5936)$ $\lvert H-1 \rightarrow L+2 \rangle + c.c.(0.0990)$
II	$1^3A_g^-$	2.92	0.996	0.064	$\lvert H \rightarrow L; H-1 \rightarrow L+1 \rangle (0.8333)$ $\lvert H-1 \rightarrow L; H-1 \rightarrow L+2 \rangle - c.c.(0.1090)$
III	$3^3B_{1g}^-$	3.39	0.465	0.017	$\lvert H \rightarrow L+3 \rangle + c.c.(0.4280)$ $\lvert H-1 \rightarrow L+2 \rangle + c.c.(0.3614)$
IV	$3^3A_g^-$	3.68	0.621	0.034	$\lvert H \rightarrow L+5 \rangle + c.c.(0.4915)$ $\lvert H-1 \rightarrow L+4 \rangle + c.c.(0.3220)$
V	$4^3B_{1g}^-$	4.01	2.601	0.641	$\lvert H \rightarrow L; H \rightarrow L+4 \rangle - c.c.(0.5605)$ $\lvert H \rightarrow L+1; H-1 \rightarrow L+4 \rangle - c.c.(0.1764)$
VI	$7^3B_{1g}^-$	4.67	1.017	0.114	$\lvert H \rightarrow L+1; H-5 \rightarrow L \rangle - c.c.(0.5190)$ $\lvert H \rightarrow L+1; H-1 \rightarrow L+4 \rangle - c.c.(0.2712)$
VII	$11^3A_g^-$	5.13	0.151	0.003	$\lvert H-1 \rightarrow L+1; H \rightarrow L+2 \rangle - c.c.(0.3311)$ $\lvert H-1 \rightarrow L+8 \rangle - c.c.(0.2700)$
	$11^3B_{1g}^-$	5.15	0.768	0.072	$\lvert H \rightarrow L+1; H-1 \rightarrow L+4 \rangle - c.c.(0.4913)$ $\lvert H \rightarrow L+1; H-5 \rightarrow L \rangle - c.c.(0.2874)$
	$12^3B_{1g}^-$	5.18	0.345	0.015	$\lvert H \rightarrow L+1; H-5 \rightarrow L \rangle - c.c.(0.4987)$ $\lvert H \rightarrow L+1; H-1 \rightarrow L+4 \rangle - c.c.(0.2693)$
	$12^3A_g^-$	5.19	0.148	0.003	$\lvert H-1 \rightarrow L+8 \rangle + c.c.(0.3959)$ $\lvert H \rightarrow L; H-1 \rightarrow L+3 \rangle - c.c.(0.2687)$
VIII	$13^3B_{1g}^-$	5.39	0.777	0.077	$\lvert H-1 \rightarrow L+8 \rangle + c.c.(0.3959)$ $\lvert H \rightarrow L; H-1 \rightarrow L+3 \rangle - c.c.(0.2687)$

Table XIV: Excited states contributing to the triplet absorption spectrum of nonacene computed using the MRSDCI method coupled with the standard parameters in the PPP model Hamiltonian. The rest of the information is same as that in XII.

Peak	State	E (eV)	Transition Dipole (Å)	ROS	Wave Functions
I	$1^3B_{1g}^-$	2.56	3.331	0.785	$\vert H \rightarrow L+1\,\rangle + c.c.(0.5522)$ $\vert H-1 \rightarrow L+2\,\rangle + c.c.(0.1825)$
II	$1^3A_g^-$	3.30	1.018	0.095	$\vert H \rightarrow L; H-1 \rightarrow L+1\,\rangle\ (0.8148)$ $\vert H \rightarrow L; H-1 \rightarrow L+3\,\rangle\ c.c.(0.1109)$
III	$2^3B_{1g}^-$	3.79	0.686	0.049	$\vert H \rightarrow L+3\,\rangle - c.c.(0.5156)$ $\vert H-1 \rightarrow L+2\,\rangle + c.c.(0.2173)$
	$3^3A_g^-$	3.89	0.352	0.013	$\vert H \rightarrow L; H-1 \rightarrow L+1\,\rangle\ (0.4041)$ $\vert H-1 \rightarrow L+4\,\rangle - c.c.(0.3279)$
IV	$3^3B_{1g}^-$	4.39	0.790	0.076	$\vert H-1 \rightarrow L+2\,\rangle + c.c.(0.4226)$ $\vert H \rightarrow L; H \rightarrow L; H-1 \rightarrow L+2\,\rangle + c.c.(0.2222)$
V	$4^3B_{1g}^-$	4.66	2.789	1.000	$\vert H \rightarrow L; H \rightarrow L+4\,\rangle + c.c.(0.5047)$ $\vert H-1 \rightarrow L; H \rightarrow L+5\,\rangle - c.c.(0.2034)$
VI	$6^3B_{1g}^-$	5.14	0.418	0.025	$\vert H \rightarrow L+1; H \rightarrow L+1; H-1 \rightarrow L\,\rangle + c.c.(0.4111)$ $\vert H \rightarrow L; H \rightarrow L+4\,\rangle + c.c.(0.2905)$
VII	$11^3A_g^-$	5.39	0.517	0.040	$\vert H \rightarrow L+5\,\rangle - c.c.(0.3654)$ $\vert H-1 \rightarrow L+4\,\rangle - c.c.(0.3219)$
	$7^3B_{1g}^-$	5.44	1.438	0.310	$\vert H \rightarrow L+1; H-5 \rightarrow L\,\rangle - c.c.(0.4435)$ $\vert H \rightarrow L+1; H \rightarrow L+4\,\rangle - c.c.(0.3271)$
VIII	$13^3A_g^-$	5.75	0.428	0.029	$\vert H-1 \rightarrow L+1; H \rightarrow L+2\,\rangle - c.c.(0.2992)$ $\vert H \rightarrow L; H-1 \rightarrow L+3\,\rangle - c.c.(0.2305)$

Table XV: Excited states contributing to the triplet absorption spectrum of nonacene computed using the MRSDCI method coupled with the screened parameters in the PPP model Hamiltonian. The rest of the information is same as that in XII.

Peak	State	E (eV)	Transition Dipole (Å)	ROS	Wave Functions
I	$1^3B_{1g}^-$	1.86	5.218	1.000	$\vert H \rightarrow L+1\,\rangle + c.c.(0.5919)$ $\vert H-1 \rightarrow L+2\,\rangle - c.c.(0.1143)$
II	$1^3A_g^-$	2.61	1.032	0.055	$\vert H \rightarrow L; H-1 \rightarrow L+1\,\rangle\ (0.8266)$ $\vert H-1 \rightarrow L; H \rightarrow L+2\,\rangle + c.c.(0.1122)$
III	$3^3B_{1g}^-$	3.14	0.711	0.031	$\vert H \rightarrow L+3\,\rangle + c.c.(0.4278)$ $\vert H-1 \rightarrow L+2\,\rangle - c.c.(0.3551)$
IV	$3^3A_g^-$	3.58	0.514	0.019	$\vert H \rightarrow L+6\,\rangle + c.c.(0.4657)$ $\vert H-1 \rightarrow L+4\,\rangle - c.c.(0.3453)$
V	$6^3B_{1g}^-$	4.09	2.577	0.535	$\vert H \rightarrow L; H \rightarrow L+4\,\rangle + c.c.(0.5088)$ $\vert H-1 \rightarrow L; H \rightarrow L+1; H \rightarrow L+1\,\rangle + c.c.(0.2302)$
VI	$10^3A_g^-$	4.52	0.324	0.009	$\vert H-1 \rightarrow L+1; H \rightarrow L+2\,\rangle - c.c.(0.3581)$ $\vert H \rightarrow L; H-1 \rightarrow L+3\,\rangle - c.c.(0.2788)$
	$8^3B_{1g}^-$	4.53	1.434	0.184	$\vert H \rightarrow L+1; H-6 \rightarrow L+1\,\rangle - c.c.(0.5621)$

					$\vert H-2\rightarrow L+3\,\rangle - c.c.(0.1869)$
VII	$11^3B_{1g}^-$	4.87	0.398	0.015	$\vert H\rightarrow L; H\rightarrow L; H-1\rightarrow L+2\,\rangle - c.c.(0.4361)$ $\vert H-1\rightarrow L; H-1\rightarrow L; H\rightarrow L+1\,\rangle + c.c.(0.3273)$
	$12^3A_g^-$	4.92	0.215	0.004	$\vert H-1\rightarrow L+8\,\rangle + c.c.(0.4643)$ $\vert H\rightarrow L; H-1\rightarrow L+3\,\rangle - c.c.(0.2204)$
VIII	$12^3B_{1g}^-$	5.14	0.884	0.079	$\vert H\rightarrow L+1; H-6\rightarrow L+1\,\rangle - c.c.(0.5873)$ $\vert H\rightarrow L; H-1\rightarrow L+2\,\rangle - c.c.(0.0756)$

Table XVI: Excited states contributing to the triplet absorption spectrum of decacene computed using the MRSDCI method coupled with the standard parameters in the PPP model Hamiltonian. The rest of the information is same as that in XII.

Peak	State	E (eV)	Transition Dipole (Å)	ROS	Wave Functions
I	$1^3B_{1g}^-$	2.49	3.615	1.000	$\vert H\rightarrow L+1\,\rangle - c.c.(0.5461)$ $\vert H-1\rightarrow L+2\,\rangle + c.c.(0.1918)$
II	$1^3A_g^-$	3.16	1.097	0.117	$\vert H\rightarrow L; H-1\rightarrow L+1\,\rangle\ (0.8189)$ $\vert H\rightarrow L; H-1\rightarrow L+3\,\rangle - c.c.(0.1177)$
III	$2^3B_{1g}^-$	3.62	0.800	0.071	$\vert H\rightarrow L+3\,\rangle - c.c.(0.5228)$ $\vert H-1\rightarrow L+2\,\rangle + c.c.(0.1965)$
IV	$3^3B_{1g}^-$	4.35	0.793	0.084	$\vert H-1\rightarrow L+2\,\rangle + c.c.(0.4745)$ $\vert H-1\rightarrow L+4\,\rangle - c.c.(0.1760)$
V	$4^3B_{1g}^-$	4.62	2.534	0.912	$\vert H\rightarrow L; H\rightarrow L+4\,\rangle - c.c.(0.4009)$ $\vert H\rightarrow L+7\,\rangle - c.c.(0.2788)$
VI	$6^3B_{1g}^-$	5.22	1.183	0.225	$\vert H\rightarrow L+1; H\rightarrow L+1; H-1\rightarrow L\,\rangle - c.c.(0.3604)$ $\vert H\rightarrow L+1; H-6\rightarrow L\,\rangle - c.c.(0.3314)$
VII	$11^3A_g^-$	5.42	0.493	0.040	$\vert H\rightarrow L+6\,\rangle + c.c.(0.3537)$ $\vert H-1\rightarrow L+4\,\rangle - c.c.(0.3086)$
	$8^3B_{1g}^-$	5.44	1.179	0.232	$\vert H\rightarrow L+1; H-1\rightarrow L; H-1\rightarrow L\,\rangle - c.c.(0.3928)$ $\vert H\rightarrow L+1; H-6\rightarrow L\,\rangle - c.c.(0.3365)$
VIII	$12^3A_g^-$	5.70	0.456	0.036	$\vert H-1\rightarrow L+1; H\rightarrow L+2\,\rangle - c.c.(0.3473)$ $\vert H\rightarrow L+1; H\rightarrow L+3\,\rangle - c.c.(0.2317)$

Table XVII: Excited states contributing to the triplet absorption spectrum of decacene computed using the MRSDCI method coupled with the screened parameters in the PPP model Hamiltonian. The rest of the information is same as that in XII.

Peak	State	E (eV)	Transition Dipole (Å)	ROS	Wave Functions

I	$1^3B_{1g}^-$	1.72	5.841	1.000	$\lvert H \rightarrow L+1\rangle - c.c.(0.5872)$ $\lvert H-1 \rightarrow L+2\rangle - c.c.(0.1112)$
II	$1^3A_g^-$	2.33	1.074	0.046	$\lvert H \rightarrow L; H-1 \rightarrow L+1\rangle\ (0.8198)$ $\lvert H \rightarrow L; H-1 \rightarrow L+2\rangle - c.c.(0.0986)$
III	$3^3B_{1g}^-$	2.89	0.831	0.034	$\lvert H \rightarrow L+3\rangle - c.c.(0.4352)$ $\lvert H-1 \rightarrow L+2\rangle - c.c.(0.3443)$
IV	$6^3B_{1g}^-$	3.80	2.695	0.470	$\lvert H \rightarrow L; H \rightarrow L+5\rangle - c.c.(0.5362)$ $\lvert H \rightarrow L+1; H-1 \rightarrow L+5\rangle - c.c.(0.1922)$
V	$8^3B_{1g}^-$	4.24	1.266	0.116	$\lvert H-1 \rightarrow L; H \rightarrow L+6\rangle - c.c.(0.4998)$ $\lvert H \rightarrow L+1; H-1 \rightarrow L+5\rangle - c.c.(0.3005)$
VI	$11^3B_{1g}^-$	4.70	0.791	0.050	$\lvert H \rightarrow L+1; H-1 \rightarrow L+5\rangle - c.c.(0.4721)$ $\lvert H \rightarrow L+1; H-6 \rightarrow L\rangle - c.c.(0.3044)$
	$14^3A_g^-$	4.72	0.135	0.001	$\lvert H-1 \rightarrow L+8\rangle - c.c.(0.4705)$ $\lvert H-3 \rightarrow L+5\rangle - c.c.(0.2190)$
VII	$13^3B_{1g}^-$	4.90	1.001	0.084	$\lvert H \rightarrow L+1; H-5 \rightarrow L+1\rangle - c.c.(0.3314)$ $\lvert H \rightarrow L+13\rangle - c.c.(0.3095)$
	$14^3B_{1g}^-$	4.91	0.638	0.034	$\lvert H \rightarrow L+13\rangle - c.c.(0.4517)$ $\lvert H \rightarrow L+1; H-5 \rightarrow L+1\rangle - c.c.(0.2219)$
	$15^3A_g^-$	4.91	0.162	0.002	$\lvert H-1 \rightarrow L+1; H \rightarrow L+4\rangle - c.c.(0.4666)$ $\lvert H-1 \rightarrow L+1; H-2 \rightarrow L+2\rangle\ (0.4449)$